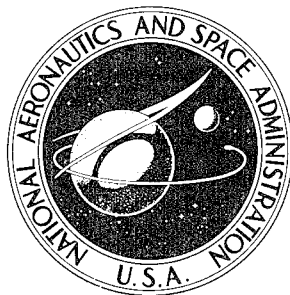


NASA TECHNICAL NOTE



NASA TN D-4916

NASA TN D-4916

19960411 007

POSTFLIGHT OPTICAL EVALUATION OF
THE RIGHT-HAND AND LEFT-HAND WINDOWS
OF GEMINI MISSIONS IV, V, VI, AND VII

*by George P. Bonner, Michael F. Heidt, Carl L. Kotila,
John A. Lintott, John E. Novotny, James W. Shafer,
and Roy C. Stokes*

*Manned Spacecraft Center
Houston, Texas*

DEPARTMENT OF DEFENSE
PLASTICS TECHNICAL EVALUATION CENTER
PICATINNY ARSENAL, DOVER, N. J.

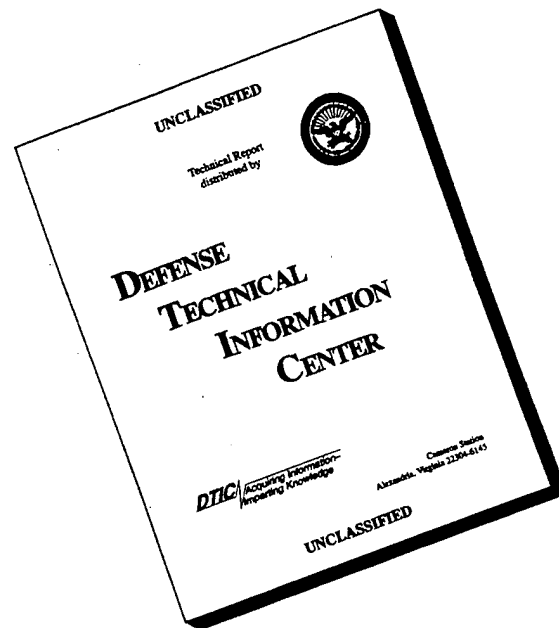
NATIONAL AERONAUTICS AND SPACE ADMINISTRATION • WASHINGTON, D. C. • DECEMBER 1968

DISTRIBUTION STATEMENT A

Approved for public release;
Distribution Unlimited

PLASTIC 11871

DISCLAIMER NOTICE



THIS DOCUMENT IS BEST QUALITY AVAILABLE. THE COPY FURNISHED TO DTIC CONTAINED A SIGNIFICANT NUMBER OF PAGES WHICH DO NOT REPRODUCE LEGIBLY.

ABSTRACT

<Transmission and relative resolution measurements were made before cleaning, and transmission, schlieren, relative resolution, and interferometric measurements were made after cleaning, on the right-hand and left-hand windows of Gemini spacecraft G-IV to G-VII. Chemical analyses of the contamination cleaned from the windows show that the primary constituent is amorphous silica.>

CONTENTS

Section	Page
SUMMARY	1
INTRODUCTION	1
SYMBOLS	1
WINDOW SPECIFICATIONS	2
CHEMICAL ANALYSIS OF THE CONTAMINATION ON THE SPACECRAFT WINDOWS	2
Test Procedure	4
Discussion of Results	6
CONCLUSIONS	8

TABLES

Table		Page
I	G-IV CHEMICAL ANALYSIS	9
II	G-V CHEMICAL ANALYSIS	10
III	G-VI CHEMICAL ANALYSIS	11
IV	G-VII CHEMICAL ANALYSIS	12
V	ABLATION MATERIALS CHEMICAL ANALYSIS	13
VI	RESOLUTION MEASUREMENTS	14
VII	WAVE-FRONT DEVIATIONS	14

FIGURES

Figures		Page
1	Cross section of Gemini window	15
2	Contamination on windows, G-IV	
	(a) Right window	16
	(b) Left window	16
3	Contamination on windows, G-V	
	(a) Right window	17
	(b) Left window	17
4	Contamination on windows, G-VI	
	(a) Right window	18
	(b) Left window	18
5	Contamination on windows, G-VII	
	(a) Right window	19
	(b) Left window	19
6	Schlierengraph field of view with horizontal knife edge	20
7	Schlierengraph of clean windows, G-V	
	(a) Right window	21
	(b) Left window	21
8	Schlierengraph of clean windows, G-VI	
	(a) Right window	22
	(b) Left window	22
9	Schlierengraph of clean windows, G-VII	
	(a) Right window	23
	(b) Left window	23
10	Photograph with 1400-mm focal-length telescope and camera	
	(a) An NBS resolution chart	24
	(b) A USAF bar chart	24

Figures		Page
11	Photographs of NBS resolution charts, G-IV	
	(a) Through dirty right window	25
	(b) Through clean right window	25
	(c) Through dirty left window	26
	(d) Through clean left window	26
12	Photographs of NBS resolution charts, G-V	
	(a) Through dirty right window	27
	(b) Through clean right window	27
	(c) Through dirty left window	28
	(d) Through clean left window	28
13	Photographs of USAF bar charts, G-VI	
	(a) Through dirty right window	29
	(b) Through clean right window	29
	(c) Through dirty left window	30
	(d) Through clean left window	30
14	Photographs of USAF bar charts, G-VII	
	(a) Through dirty right window	31
	(b) Through clean right window	31
	(c) Through dirty left window	32
	(d) Through clean left window	32
15	Interferograms, G-IV	
	(a) Clean right window	33
	(b) Clean left window	33
16	Interferograms, G-V	
	(a) Clean right window	34
	(b) Clean left window	34
17	Interferograms, G-VI	
	(a) Clean right window	35
	(b) Clean left window	35
18	Interferograms, G-VII	
	(a) Clean right window	36
	(b) Clean left window	36

Figures		Page
19	Location of vertical and lateral scans on right windows	37
20	Location of vertical and lateral scans on left windows	38
21	Percent transmission versus lateral displacement of dirty right window for G-V, G-VI, and G-VII	39
22	Percent transmission versus lateral displacement of dirty left window for G-IV, G-VI, and G-VII	39
23	Percent transmission versus vertical displacement of dirty right window for G-VI and G-VII	40
24	Percent transmission versus vertical displacement of dirty left window for G-IV, G-VI, and G-VII	40
25	Percent transmission versus wavelength of dirty right window for G-IV to G-VII	41
26	Percent transmission versus wavelength of dirty left window for G-IV to G-VII	41
27	Percent transmission versus wavelength and angle of incidence for clean right window	42
28	Percent transmission versus wavelength and angle of incidence for clean left window	42

POSTFLIGHT OPTICAL EVALUATION OF THE RIGHT-HAND AND LEFT-HAND WINDOWS OF GEMINI MISSIONS IV, V, VI, AND VII

By George P. Bonner, Michael F. Heidt, Carl L. Kotila,
John A. Lintott, John E. Novotny, James W. Shafer,
and Roy C. Stokes
Manned Spacecraft Center

SUMMARY

Transmission and relative resolution measurements were made before cleaning; and transmission, schlieren, relative resolution, and interferometric measurements were made after cleaning, on the right-hand and left-hand windows of the Gemini spacecraft G-IV to G-VII. Tests made before cleaning indicate that the left windows were more contaminated on spacecraft G-IV to G-VI, while the right window was more contaminated on spacecraft G-VII. Chemical analyses were conducted on the residue that was removed from the outer surfaces of each window and from the inner surface of the right window outer pane. The results of chemical analyses were similar on all flights. The primary constituent of the contamination is amorphous silica.

INTRODUCTION

The principal experimenters for particular Gemini experiments wanted the optical properties of the windows defined. Consequently, the Office of Space Science and Applications required that the optical properties of the spacecraft windows were to be measured and documented after each flight. The complex nature of the assembly, the presence of the coatings, and the uncertainty in mounting required that the properties be measured rather than analytically assessed.

Relative resolution was determined by photographing either a National Bureau of Standards (NBS) resolution chart or a U.S. Air Force (USAF) bar chart through the window. Schlierengraphs were obtained showing nonuniform deviations of parallel light through the window. Interferograms were obtained to determine the wave-front distortions that were caused by the windows. Spectral transmission was measured by noting the loss of intensity of a parallel monochromatic beam of light after passing through the window.

SYMBOLS

I_k incident voltage

I_λ incident energy

IN_k	incident noise
k	index of summation
n	number of terms in summation
P_I	probable error in incident voltage
P_T	probable error in transmitted voltage
PE_T	probable error in percent transmitted
T_k	transmitted voltage
T_λ	transmitted energy
TN_k	transmitted noise
θ	angle of incidence
λ	wavelength
σ_I	standard deviation in incident voltage
σ_T	standard deviation in transmitted voltage

WINDOW SPECIFICATIONS

The window of the Gemini spacecraft was a multilayer assembly consisting of three panes (fig. 1) with an antireflectance coating on five of the six sides. Military specifications MIL-O-13830 and JAN-G-174 formed the base line for the optical quality of the Gemini windows. Additional requirements for the right (optical) window called for flatness to 1.5 wavelengths (540 $m\mu$) over a 5-inch-diameter circle, 3.0 wavelengths over the remainder of the window, and light deviation in each pane not to exceed 1 minute of arc.

CHEMICAL ANALYSIS OF THE CONTAMINATION ON THE SPACECRAFT WINDOWS

The first hint of window contamination was on the Gemini spacecraft G-3 right-hand window. Although the window was cleaned before delivery to the optics laboratory, a spot of contamination about 0.5 cm in diameter remained. The contamination material was removed and analyzed with a spectrograph. A cursory examination of the plate showed both silica and sodium lines. This contamination was attributed to heat-shield ablation products deposited during reentry.

A circumstance during the next scheduled Gemini flight invalidated the conclusions for the source of contamination on the G-3 windows. During extravehicular activity on the G-IV flight, the command pilot reported that the pilot had inadvertently brushed against the left-hand window and smeared it. This was the first indication that the contamination was placed upon the windows during the ascent stage rather than the descent stage of the flight. Both pilots reported that each window tended to burn upon reentry with an "orange peel" effect. The pilot reported difficulty in viewing the launch vehicle because of dirty windows.

Pilots on succeeding Gemini flights also reported window contamination. The command pilot, during the G-V flight, said that he saw globules strike the window during the nose-fairing jettison stage. The pilot of the G-VI said he observed a white cloud prior to staging. After staging, the cloud appeared distorted and darkened in color, he said. The G-VII crew reported similar window observations associated with staging. The command pilot reported that the coating on the G-VI window, as viewed during rendezvous, was in an amorphous state somewhat resembling model airplane cement.

Optics laboratory personnel of the Manned Spacecraft Center (MSC) were assigned the task to determine the actual chemical elements present in the deposits and to provide a logical explanation as to the possible sources of the contamination. Photographs of the G-IV to G-VII right-hand and left-hand windows (figs. 2 to 5) show the type of contamination deposited on the windows. The following observations, made before any cleaning or scraping was done to obtain samples for chemical analysis, apply to all windows:

1. The deposit was dull white to gray.
2. The material displayed a slight fluorescence when viewed under ultraviolet light.
3. Low-power microscopy indicated that some of the material could have come from the seal around the window.
4. High-power microscopy indicated the presence of two or more distinct layers of material, which appear to act as a trap to particulate matter.
5. Polarized-light microscopy indicated the presence of polarizing material.

After the preliminary examination, the windows were scraped and the residue was prepared for analysis. The G-IV windows had been washed while aboard the recovery ship; therefore, there was only one sample per window. At the request of optics personnel, the windows from succeeding spacecraft were covered and sent to the optics laboratory as soon as possible after recovery. The windows were not washed or otherwise handled. A sample was taken from the windows upon arrival in the laboratory, the windows were washed with distilled water, and another sample taken. Then the windows were cleaned completely by scraping and washing with water and alcohol. The chemical analyses of the samples showed which elements of the contamination were loosely bonded or soluble in water. Most of the water soluble elements were attributed to contamination from the sea water.

Methods of chemical analyses used on the G-IV samples included emission spectroscopy, X-ray diffraction analysis, electron probe spectroscopy, infrared spectrophotometry, ring-oven studies, and neutron-activation analysis. Emission spectroscopy was the most effective means of analysis, and the composition of the contamination (tables I to IV) was compiled from the results obtained with this instrument. The other methods of analysis support the results obtained from the emission spectrograph.

Table V presents the spectrographic analysis of all the ablative materials located externally to the spacecraft. The patching material, the silicone rubber sponge gasket, and the laminated fiber-glass materials were eliminated as major contributors to the window contamination. These materials are solids, and indications are that the temperatures at the geometrical locations of these materials on the spacecraft do not support a theory that they could have reached an ablation stage during the launch phase. On the other hand, DC-325, the ablation material for the nose-cone fairing, and RTV, painted about the spacecraft at many places, are more likely contributors. With few exceptions (such as the presence of antimony and silver), all trace elements and silica can be attributed to RTV and DC-325. Laboratory tests indicate that DC-325, when raised to a temperature in excess of 300° F, outgasses a vapor of silicone oil. At a temperature greater than 800° F, the oil vapor appears to go through a phase change depositing a milky gray film. A further increase in temperature causes the destruction of the oil and leaves a silica deposit.

Test Procedure

Spectral transmission. - A source of radiant energy is focused upon the entrance slit of a prism monochromator. The energy is dispersed into its spectrum by the prism. A portion of the spectrum is focused to illuminate the monochromator exit slit. The desired portion of the spectrum appearing at the exit slit is selected by manually rotating the prism.

The divergent monochromatic energy that passes through the exit slit is then made parallel by placing the exit slit at the focal point of an off-axis parabolic mirror. The intensity of the collimated monochromatic energy is recorded as millivolts output from a photomultiplier. The spacecraft window is then inserted into the beam, and the intensity of the transmitted energy is recorded. The ratio of the intensity of the radiant energy passing through the window to the intensity in the absence of the window is defined as the transmission.

Measurements of transmission as a function of wavelength (in 10 $m\mu$ steps in the segment of the spectrum from 350 to 1000 $m\mu$) were recorded for angles of incidence of 0°, 15°, 30°, and 45°.

A 2-inch spot in the central area of each window was selected for spectral transmission measurements at normal incidence before the windows were cleaned, in order to demonstrate the effect of the contamination upon the transmission. Transmission measurements at normal incidence as a function of lateral and vertical displacement were made across each window in 0.5-inch steps at a wavelength of 800 $m\mu$.

For each angle of incidence θ , a series of readings was taken to establish the dark-background-voltage level for the incident noise IN_k and transmitted noise TN_k . Average noise values are computed by

$$IN_{av} = \frac{1}{n} \left(\sum_{k=1}^n IN_k \right) \quad TN_{av} = \frac{1}{n} \left(\sum_{k=1}^n TN_k \right) \quad (1)$$

At each wavelength λ , a set of readings was taken to determine the incident voltage I_k and transmitted voltage T_k . Their averages are given by

$$I_{av} = \frac{1}{n} \left(\sum_{k=1}^n I_k \right) \quad T_{av} = \frac{1}{n} \left(\sum_{k=1}^n T_k \right) \quad (2)$$

To establish the voltage level representing the incident energy I_λ and transmitted energy T_λ , the dark-background level must be eliminated. Thus, I_λ and T_λ are given by the expression

$$I_\lambda = I_{av} - IN_{av} \quad T_\lambda = T_{av} - TN_{av} \quad (3)$$

By using the values of I_λ and T_λ , the percent transmission is determined by the expression

$$\text{Percent transmission} = \left(\frac{T_\lambda}{I_\lambda} \right) 100 \quad (4)$$

Statistical analysis of the data included

P_I = probable error in incident voltage

P_T = probable error in transmitted voltage

σ_I = standard deviation in incident voltage

σ_T = standard deviation in transmitted voltage

With these properties computed, the probable error in percent transmitted PE_T is given by

$$PE_T = \left[\left(\frac{P_I}{I_{av}} 100 \right)^2 + \left(\frac{P_T}{T_{av}} 100 \right)^2 \right]^{1/2} \quad (5)$$

This calculation shows that the random error in the data was not greater than 0.6 percent.

Schlieren test. - Each window was positioned normal to the parallel light beam in a schlieren system. Any deviation of the parallel beam of light appeared in the schlierengraphs as variations in light intensity. The variations indicated irregular surface conditions, variations of the index of refraction, nonparallelism of the surfaces, and flaws in the window materials. Schlierengraphs are shown in figures 6 to 9.

Resolution. - In all optical experiments, both scientific and photographic, the window must be considered as an integral part of the optical train. Any loss in resolution or any distortion introduced into the wave fronts should be evaluated. Photographs of NBS resolution charts (G-IV and G-V) and USAF bar charts (G-VI and G-VII) were taken with a 1400-mm focal-length telescope serving as a lens for a 35-mm camera. The telescope was used on the surface-photography experiment and imposed the most stringent resolution requirements on Gemini. The chart was photographed with and without the window inserted in the field of view of the camera. Photographs of the charts are shown in figures 10 to 14. These photographs were not used to determine the relative loss of resolution. The relative loss of resolution due to the windows was obtained by microscopic examination of the original negatives.

Interferometer. - A Mach-Zehnder-type interferometer with a 6-inch clear aperture was used for the interferometric study. The advantage of the Mach-Zehnder is that the wave front passes through the window only once, thereby eliminating the possibility of double-pass cancellations. Wedge angle, changes in the index of refraction, variations in surface flatness, and nonparallelism of one pane relative to the other panes are contributing factors to wave-front deviations that are determined by interferograms. Photographs showing interference patterns of right and left windows are shown in figures 15 to 18.

Discussion of Results

Transmission. - The results of the transmission measurements, graphically illustrated in this report (figs. 19 to 24), show the transmission through the dirty windows as a function of displacement; the transmission through the dirty windows as a function of wavelength; and the transmission through the clean windows as a function of wavelength and angle of incidence.

Transmission measurements of the dirty windows as a function of lateral and vertical displacement were made in 0.5-inch steps for normal incidence and at $800\text{ m}\mu$. The locations of the lateral and vertical scans across the right and left windows are shown in figures 19 and 20, respectively. The lateral scans across the right and left windows, figures 21 and 22, respectively, were taken toward the axis of symmetry. The vertical scan across the right and left windows, figures 23 and 24, respectively, were taken from top to bottom.

Measurements were made through each dirty window to illustrate the effect of contamination on spectral transmission at normal incidence. Values were obtained over the spectral range from 350 to $1000\text{ m}\mu$ in $10\text{-m}\mu$ steps. Data for the right windows are plotted in figure 25; data for the left windows are plotted in figure 26. The loss in transmission due to contamination increased with decreasing wavelength. A comparison of figures 25 and 26 indicated that the left window was more contaminated on G-IV, G-V, and G-VI while the right window was more contaminated on G-VII.

Measurements were taken to illustrate the change in transmission as a function of wavelength and angle of incidence through the clean windows. Values were obtained over the spectral range from 350 to $1000\text{ m}\mu$, in increments of $10\text{ m}\mu$, for angles of incidence of 0° , 15° , 30° , and 45° . Because the transmission at each angle of incidence for the G-IV, G-V, G-VI, and G-VII right and left windows agreed with each other within ± 2 percent, representative curves were plotted as shown in figures 27 and 28 for right and left windows, respectively. A comparison of the curves indicated that the loss in transmission with increasing angle of incidence was greater for increasing wavelengths.

Schlieren. - Results of the schlieren study are shown in schlierengraphs (figs. 6 to 9). Figure 6 shows the uniform field of the open schlieren. Figures 7(a), 8(a), and 9(a) show the clean right windows inserted into the beam. Figure 7(b) (the G-V left window) shows a material flaw in the lower right-hand corner. The dark areas in figures 7(b), 8(b), and 9(b) (the G-V, G-VI, and G-VII clean left windows) are caused by either a wedge angle and/or a deviation from surface flatness.

Resolution. - The NBS resolution chart (fig. 10(a)), and the USAF bar chart (fig. 10(b)) were taken with the telescope serving as a lens for the 35-mm camera. The charts, viewed through the dirty right windows, are shown in figures 11(a), 12(a), 13(a), and 14(a). The charts viewed through the clean right windows are shown in figures 11(b), 12(b), 13(b), and 14(b). The resolution charts (figs. 11(c), 12(c), 13(c), and 14(c)) were taken through the dirty left windows. The charts, viewed through the clean left windows, are shown in figures 11(d), 12(d), 13(d), and 14(d). Results of the resolution studies are presented in table VI. The table gives both the percent loss in resolution through the dirty and clean windows and the percent degradation due to the contamination.

Interferometer. - Interferograms of the right windows are shown in figures 15(a), 16(a), 17(a), and 18(a); and the interferograms of the left windows are shown in figures 15(b), 16(b), 17(b), and 18(b). Wave-front deviation ranged from 0.2 to 1 wave for the right windows, and from 1 to 14 waves for the left windows. The maximum and average deviations for each window are presented in table VII. The values given are relative to the mercury green line at $546.1\text{ m}\mu$.

CONCLUSIONS

The principal material found on the Gemini windows was a silicone oil. During launch, when the temperature exceeded 300° F, the DC-325 covering the nose-cone fairing began to ablate and released a vapor of silicone oil that was deposited on the windows. At 800° F, the silicone-oil film passed through a phase change and appeared as a cloudy, milky, translucent substance. Upon reentry, the temperature reached a point where the silicone oil oxidized, changing the nature of the silicone into an opaque film that became fused to the window. The contamination that was deposited on the outer surface of the windows reduced the properties of the windows as noted:

1. Spectral transmission ranged from 17 to 50 percent lower than the clean window.
2. Degradation of resolution ranged from 0 to 60 percent.

The schlieren, interferometric, and resolution studies demonstrated that the optical quality of the clean right windows was better by an order of magnitude than the quality which was required by the specifications that were established for the right windows. The transmission measurements on both clean and dirty windows revealed a decrease in transmission with increasing wavelength, due to the antireflectance coatings. This effect is greater at increasing angles of incidence because of the angular dependence of the coatings. Tests on the dirty windows indicated a decrease in overall transmission, but with a greater decrease at the shorter wavelengths, because of increased scattering and absorption.

Manned Spacecraft Center
National Aeronautics and Space Administration
Houston, Texas, August 12, 1968
923-50-10-06-72

TABLE I. - G-IV CHEMICAL ANALYSIS

Element	Left window (a)	Right window (a)
Aluminum	3	4
Antimony	1	1
Boron	1	1
Calcium	3	3
Copper	3	3
Iron	1	1
Lead	4	4
Magnesium	2	2
Manganese	-	-
Nickel	3	-
Silica	>>1	>>1
Silver	3	3
Sodium	4	4
Tin	4	2
Zinc	-	4

^aThe value 1 is major and is greater than 10 percent, 2 is medium and is 1 to 10 percent, 3 is light and is less than 1 percent, and 4 is very light and is less than 0.1 percent.

TABLE II. - G-V CHEMICAL ANALYSIS

Element	Before washing (a)		After washing (a)	
	Left window	Right window	Left window	Right window
Aluminum	1	1	1	2
Antimony	2	2	2	4
Boron	1	1	1	2
Calcium	1	1	2	3
Chromium	3	3	-	-
Cobalt	-	3	-	-
Copper	1	1	1	2
Iron	1	1	1	3
Lead	1	1	1	4
Magnesium	1	1	1	3
Manganese	4	4	4	-
Molybdenum	-	4	-	-
Nickel	3	3	-	-
Silica	>1	>1	>1	-
Silver	2	3	2	4
Sodium	2	3	4	4
Tin	3	3	3	4
Titanium	3	3	3	4
Zinc	3	3	-	-

^aThe value 1 is major and is greater than 10 percent, 2 is medium and is 1 to 10 percent, 3 is light and is less than 1 percent, and 4 is very light and is less than 0.1 percent.

TABLE III. - G-VI CHEMICAL ANALYSIS

Element	Before washing (a)		After washing (a)	
	Right window	Left window	Right window	Left window
Aluminum	4	4	<4	<4
Antimony	4	4	4	4
Boron	3	2	3	2
Calcium	2	2	4	4
Chromium	4	4	<4	<4
Cobalt	3	3	4	-
Copper	4	4	4	4
Iron	2	2	3	3
Lead	4	4	4	4
Magnesium	2	2	4	4
Manganese	4	<4	<4	<4
Molybdenum	4	-	4	-
Nickel	3	3	<4	<4
Silicon	1	1	1	1
Silver	4	4	<4	<4
Sodium	2	2	<4	<4
Strontium	4	4	-	-
Tin	4	4	4	4
Titanium	4	4	-	-
Zinc	<4	<4	<4	<4

^aThe value 1 is major and is greater than 10 percent, 2 is medium and is 1 to 10 percent, 3 is light and is less than 1 percent, and 4 is very light and is less than 0.1 percent.

TABLE IV. - G-VII CHEMICAL ANALYSIS

Element	Before washing (a)		After washing (a)			
	Right window	Left window	Right window	Left window	Right window (back side)	Left window (black paint ^b)
Aluminum	4	4	<4	<4	4	4
Antimony	3	3	4	4	-	<4
Boron	3	3	3	4	4	3
Calcium	3	2	4	4	3	2
Chromium	<4	4	-	-	<4	< <4
Cobalt	-	4	-	-	4	4
Copper	4	4	<4	<4	<4	<4
Iron	3	3	4	4	4	3
Lead	4	4	<4	<4	<4	4
Magnesium	4	2	<4	4	4	2
Manganese	-	4	-	-	-	4
Molybdenum	-	<4	-	-	-	-
Nickel	-	4	-	-	4	4
Silicon	1	1	1	1	1	1
Silver	4	4	4	4	4	4
Sodium	3	2	-	-	4	4
Strontium	-	4	-	-	-	4
Tin	4	4	<4	<4	<4	<4
Titanium	4	4	<4	<4	4	<4
Zinc	4	4	-	-	-	-

^aThe value 1 is major and is greater than 10 percent, 2 is medium and is 1 to 10 percent, 3 is light and is less than 1 percent, and 4 is very light and is less than 0.1 percent.

^bThin strips of black paint were placed on both the inner and outer windows and were used to orient the spacecraft to the horizon.

TABLE V. - ABLATION MATERIALS CHEMICAL ANALYSIS

Element	RTV (a)	DC-325 (a)	Patch (a)	Gasket (a)	Laminate (a)
Aluminum	2	3	1	1	>1
Antimony	-	-	-	-	-
Boron	-	>1	>1	-	>1
Calcium	3	3	1	3	>1
Copper	3	3	3	3	2
Iron	>1	4	1	1	1
Lead	1	-	3	-	3
Magnesium	3	3	4	3	>1
Manganese	2	4	-	-	-
Nickel	-	-	-	-	-
Silica	>1	>1	1	2	1
Silver	-	-	4	4	-
Sodium	2	>1	2	-	1
Tin	1	-	-	-	-
Zinc	3	-	3	3	3

^aThe value 1 is major and is greater than 10 percent, 2 is medium and is 1 to 10 percent, 3 is light and is less than 1 percent, and 4 is very light and is less than 0.1 percent.

TABLE VI. - RESOLUTION MEASUREMENTS

Flight	Percent loss in resolution				Percent degradation by contamination	
	Right dirty	Right clean	Left dirty	Left clean	Right	Left
G-IV	50	15	75	40	41	58
G-V	29	18	29	29	13	0
G-VI	17	10	72	45	8	51
G-VII	63	20	75	58	54	40

TABLE VII. - WAVE-FRONT DEVIATIONS

Flight	Through right window		Through left window	
	Maximum	Average	Maximum	Average
G-IV	0.38	0.25	10.25	5.5
G-V	2.6	1.1	18.8	12.4
G-VI	.75	.40	17.0	12.0
G-VII	.20	.15	14 waves over a 6-inch aperture	14 waves over a 6-inch aperture

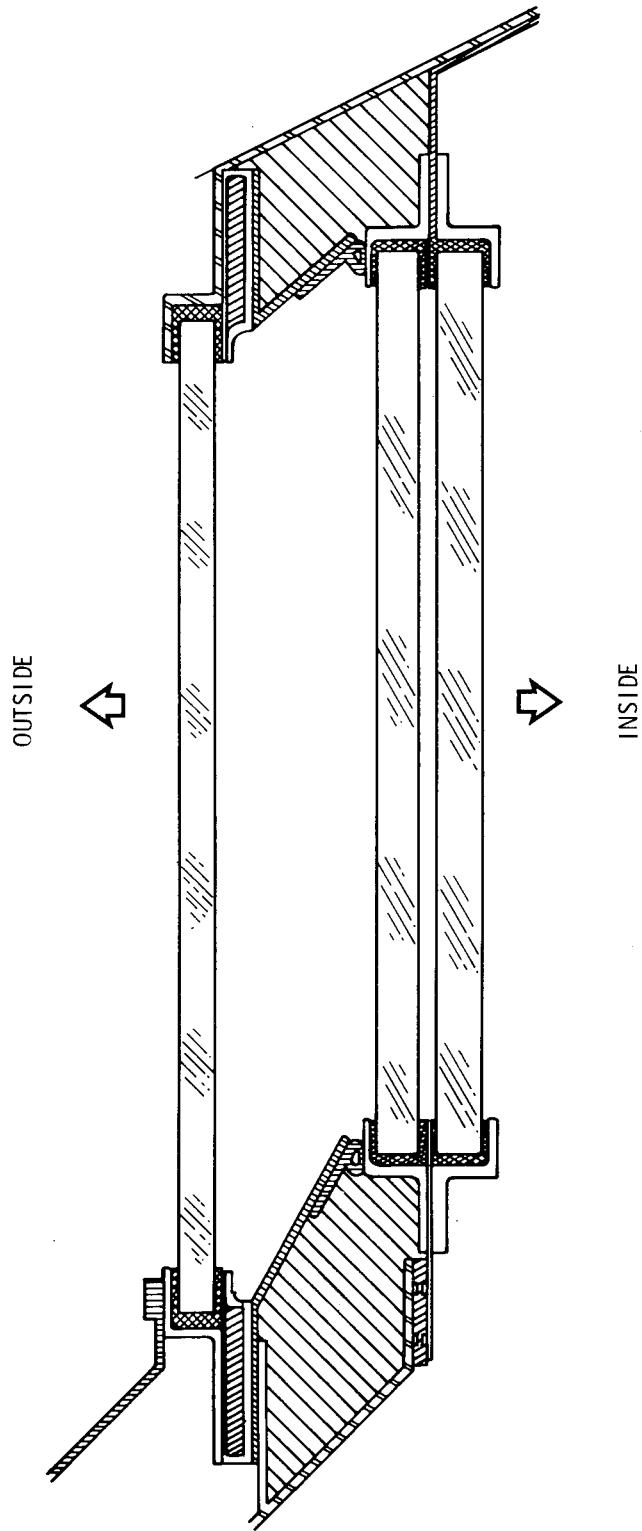
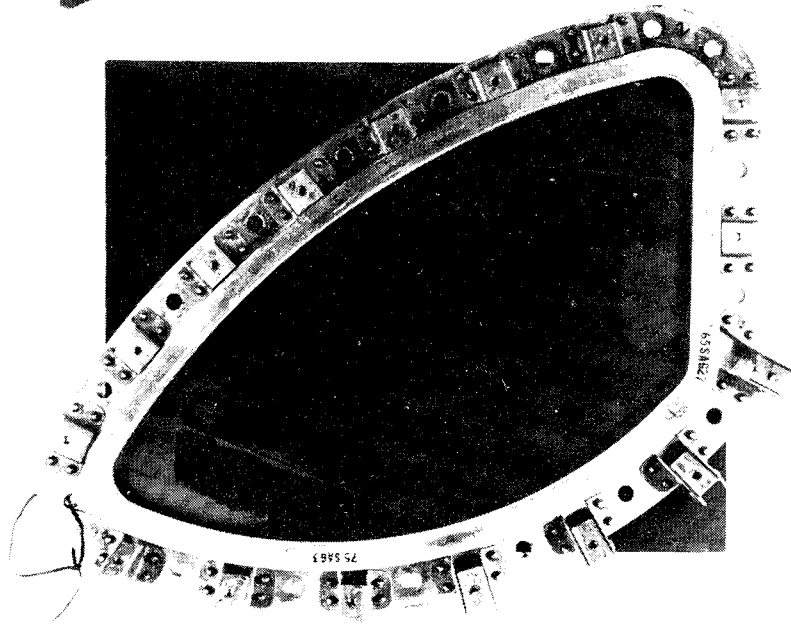
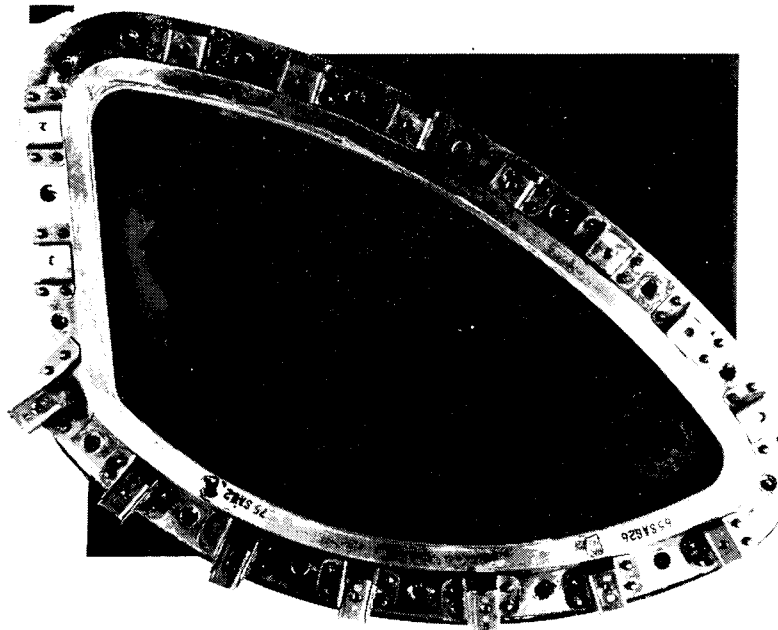


Figure 1. - Cross section of Gemini window.

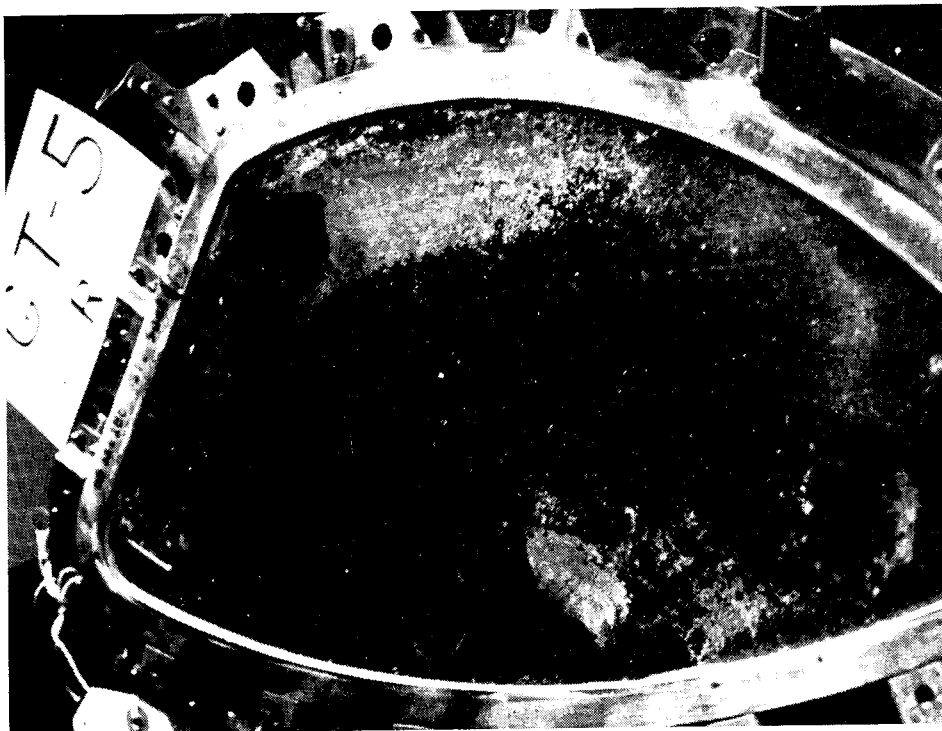


(a) Right window.

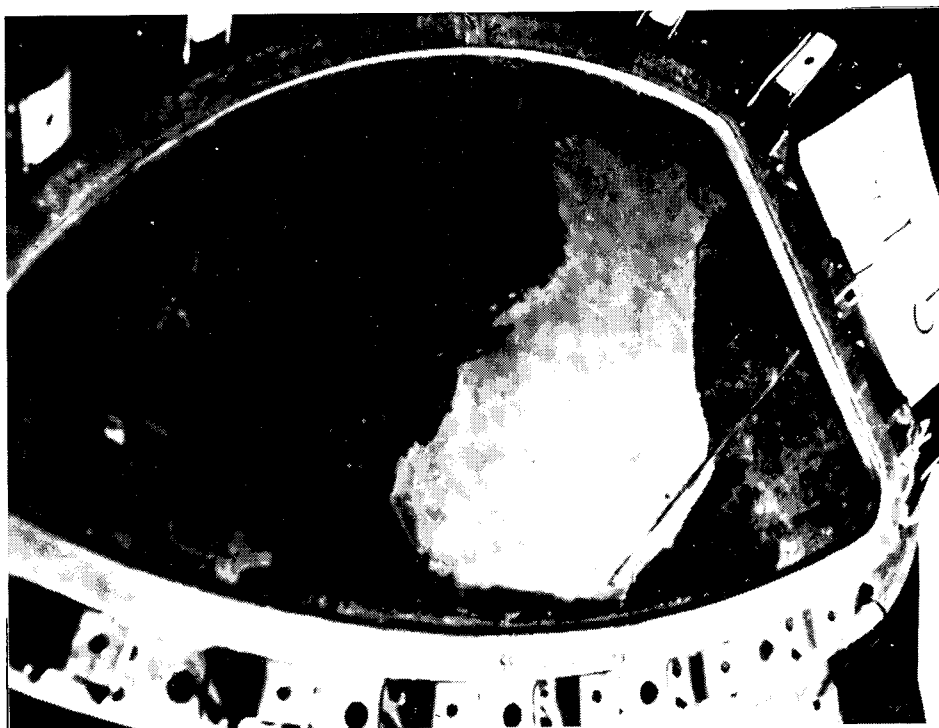


(b) Left window.

Figure 2. - Contamination on windows, G-IV.

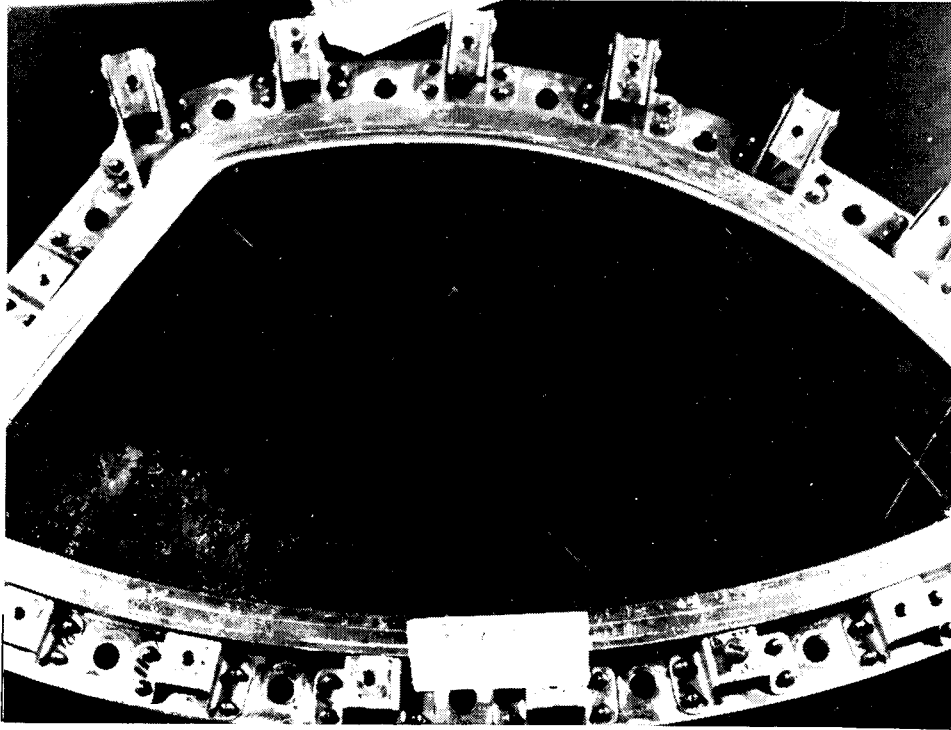


(a) Right window.

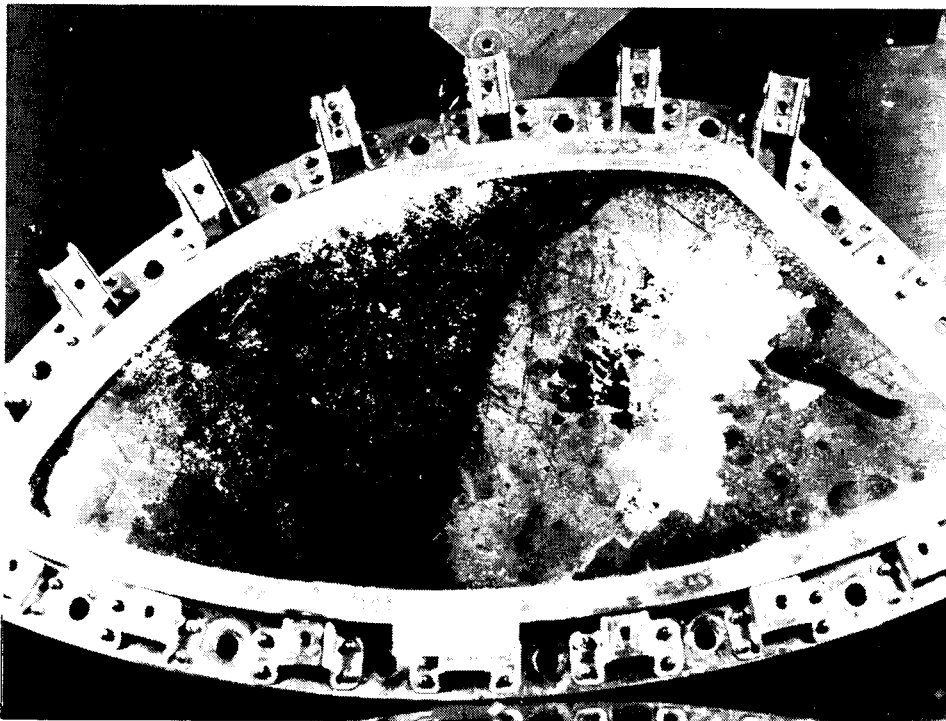


(b) Left window.

Figure 3. - Contamination on windows, G-V.

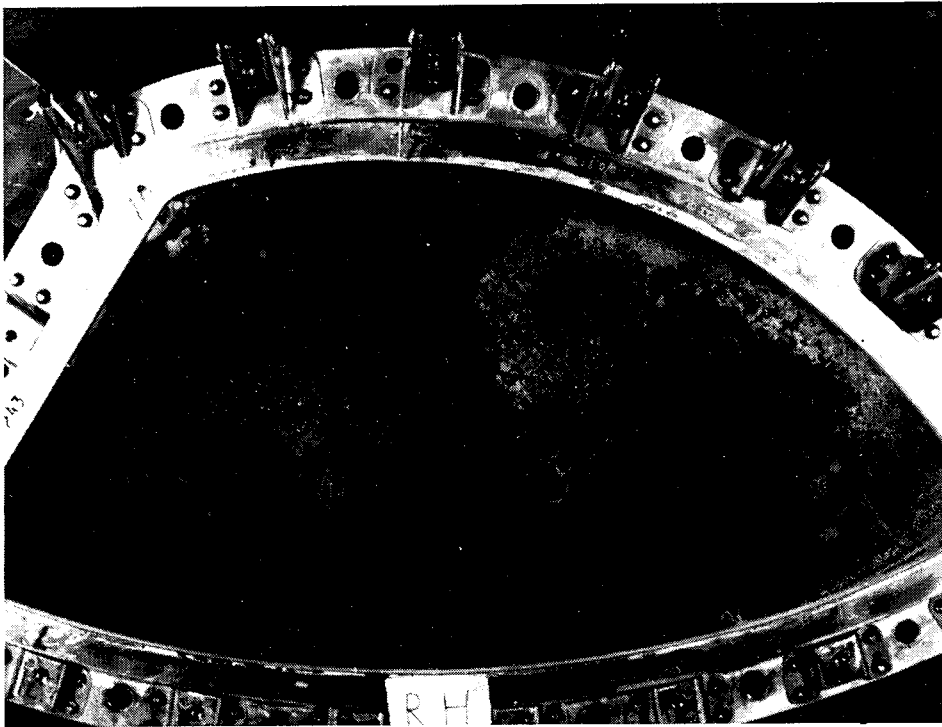


(a) Right window.

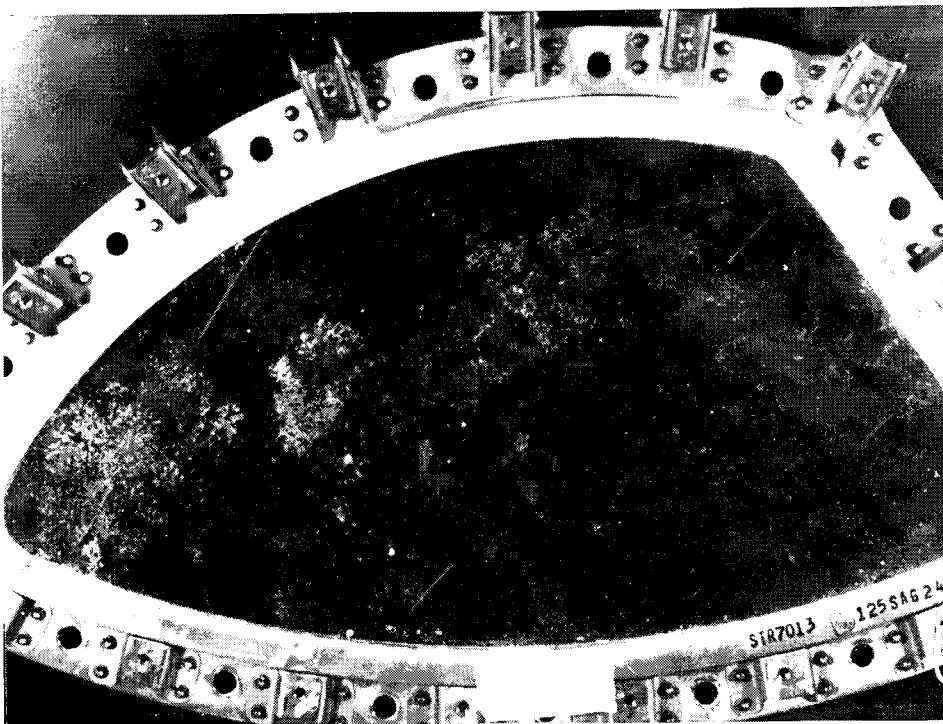


(b) Left window.

Figure 4. - Contamination on windows, G-VI.



(a) Right window.



(b) Left window.

Figure 5. - Contamination on windows, G-VII.

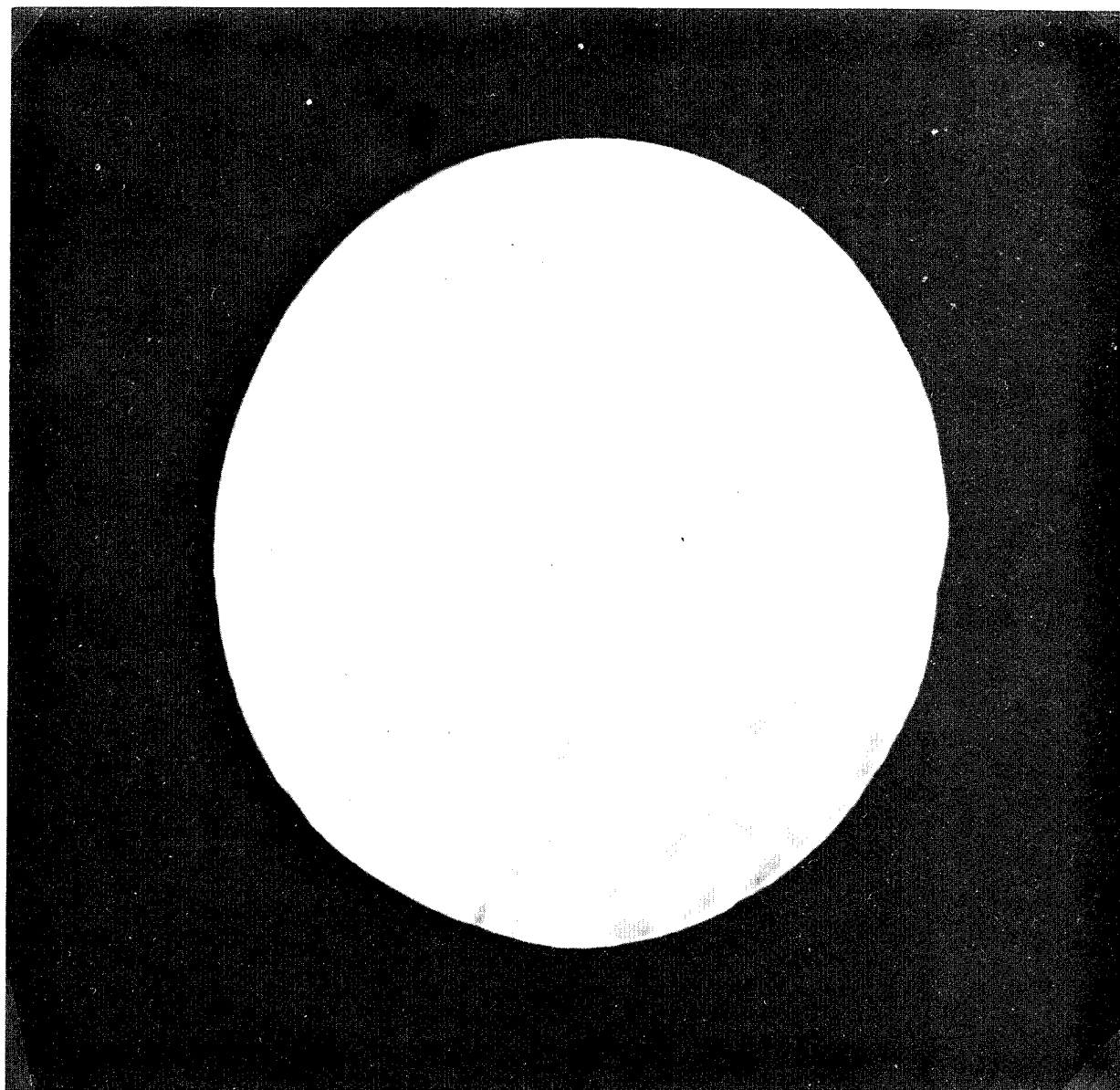


Figure 6. - Schlierengraph field of view with horizontal knife edge.



(a) Right window.

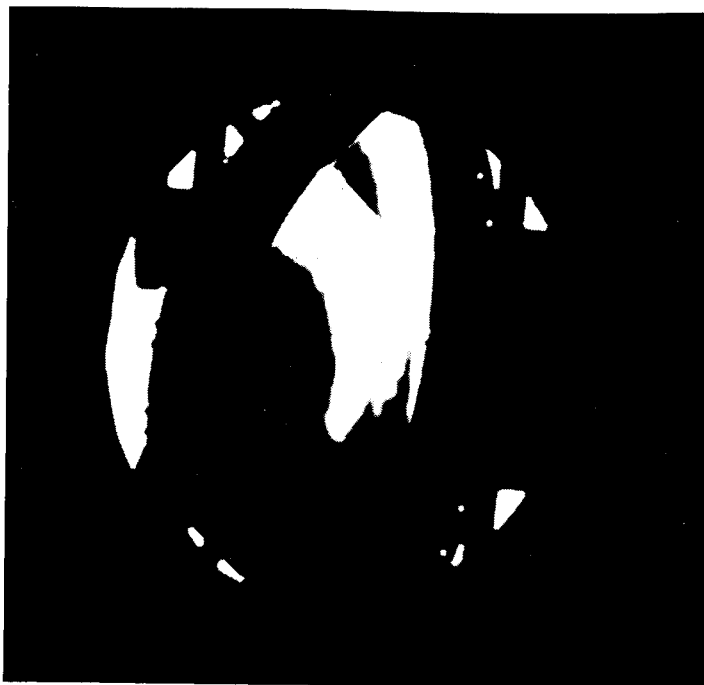


(b) Left window.

Figure 7. - Schlierengraph of clean windows, G-V.

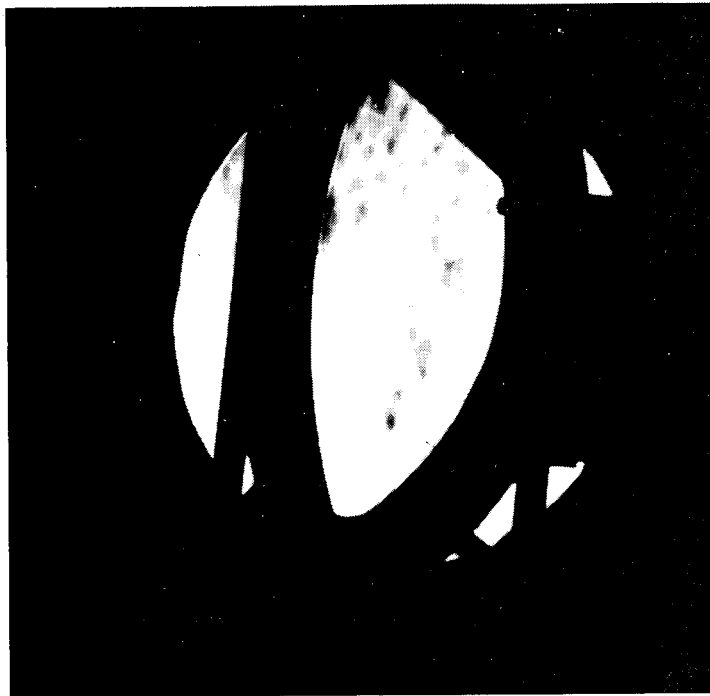


(a) Right window.

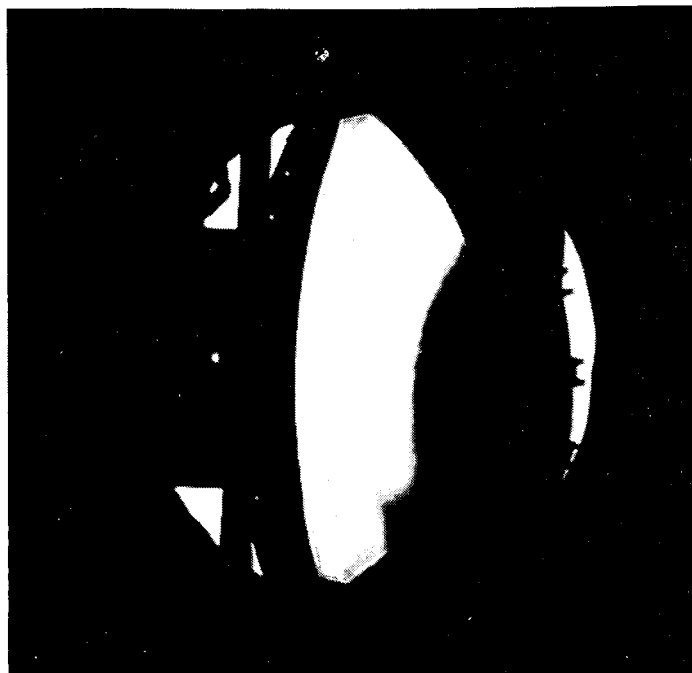


(b) Left window.

Figure 8. - Schlierengraph of clean windows, G-VI.

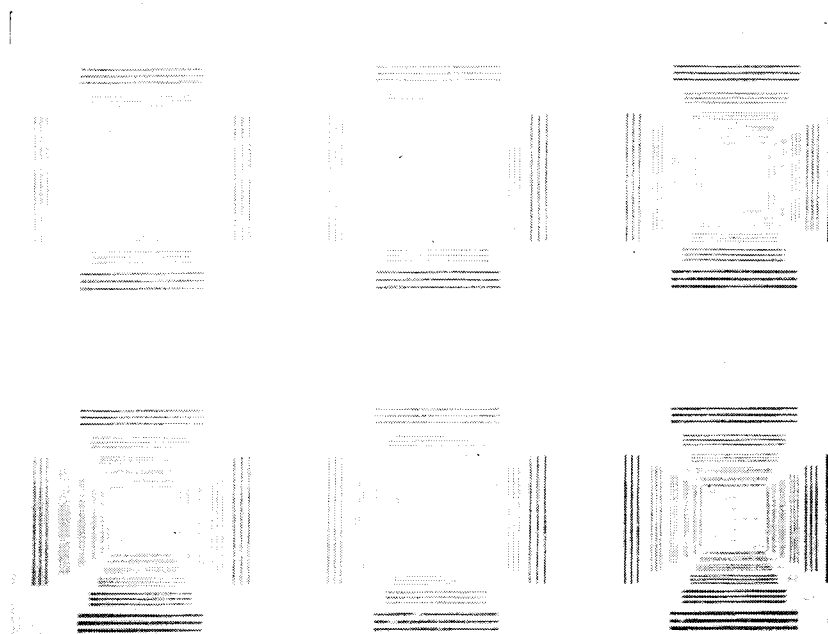


(a) Right window.

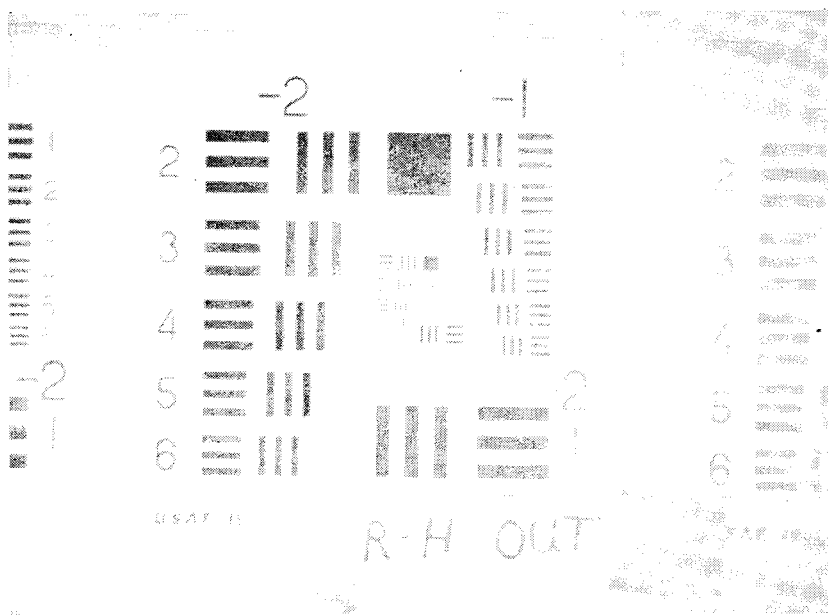


(b) Left window.

Figure 9. - Schlierengraph of clean windows, G-VII.

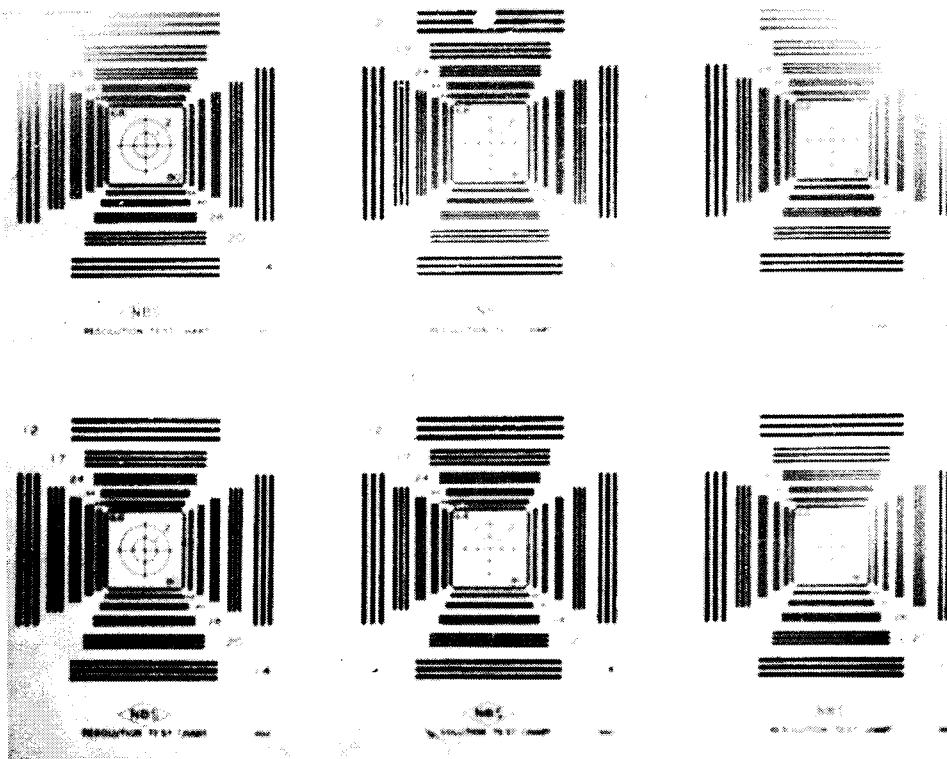


(a) An NBS resolution chart.

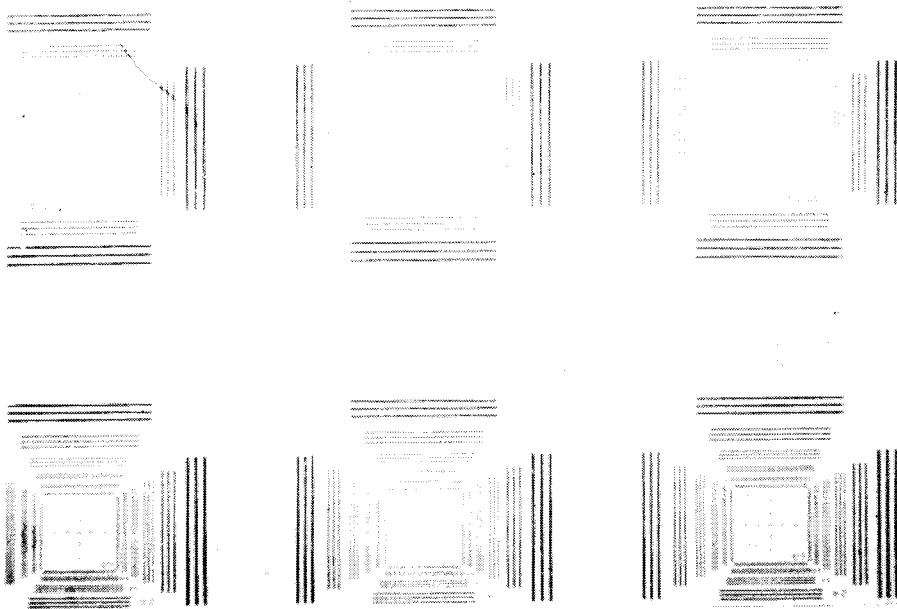


(b) A USAF bar chart.

Figure 10. - Photograph with 1400-mm focal-length telescope and camera.

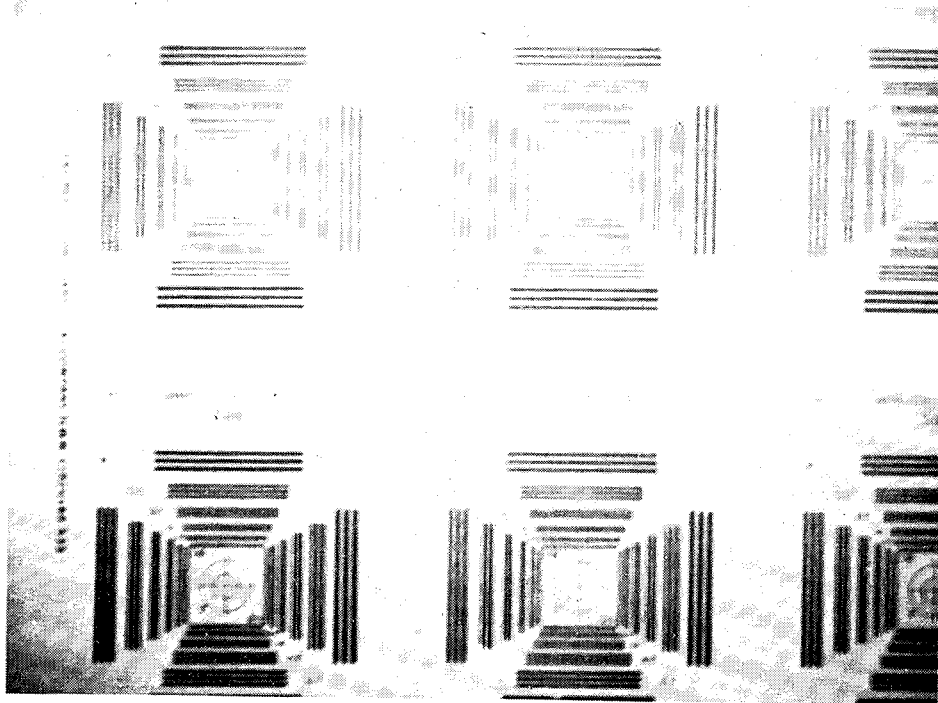


(a) Through dirty right window.

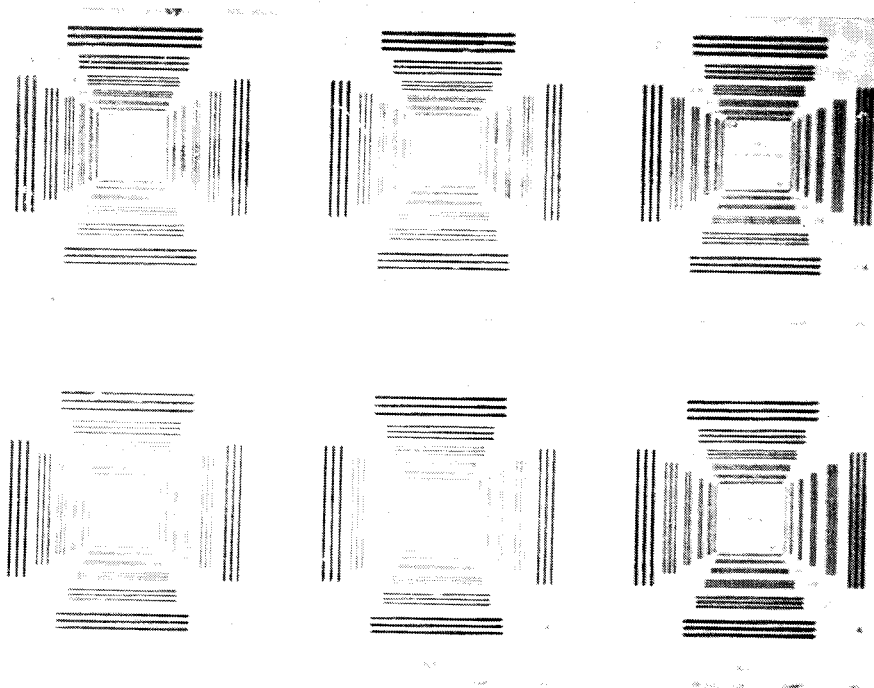


(b) Through clean right window.

Figure 11. - Photographs of NBS resolution charts, G-IV.

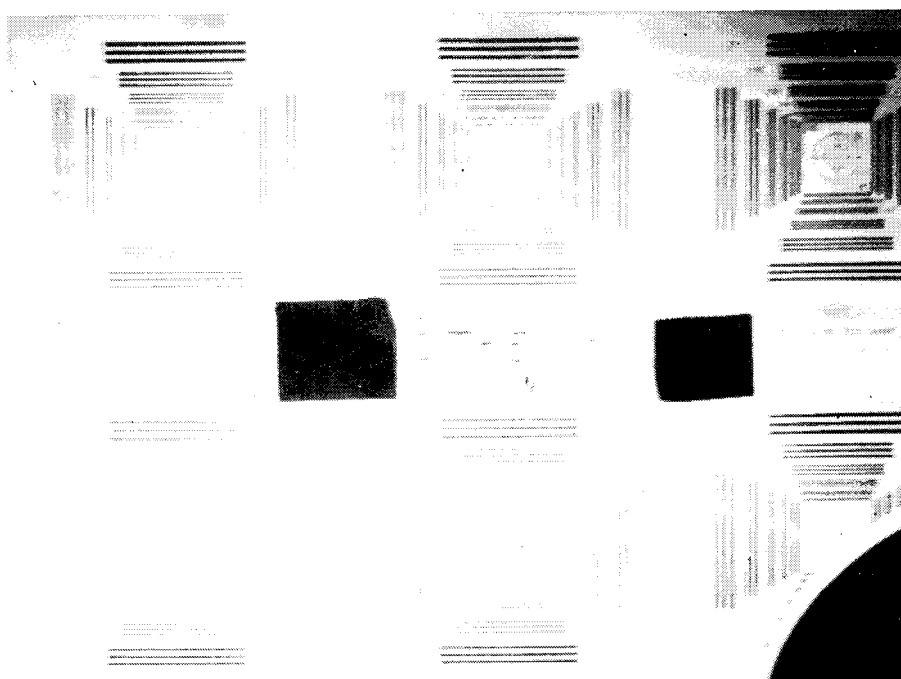


(c) Through dirty left window.

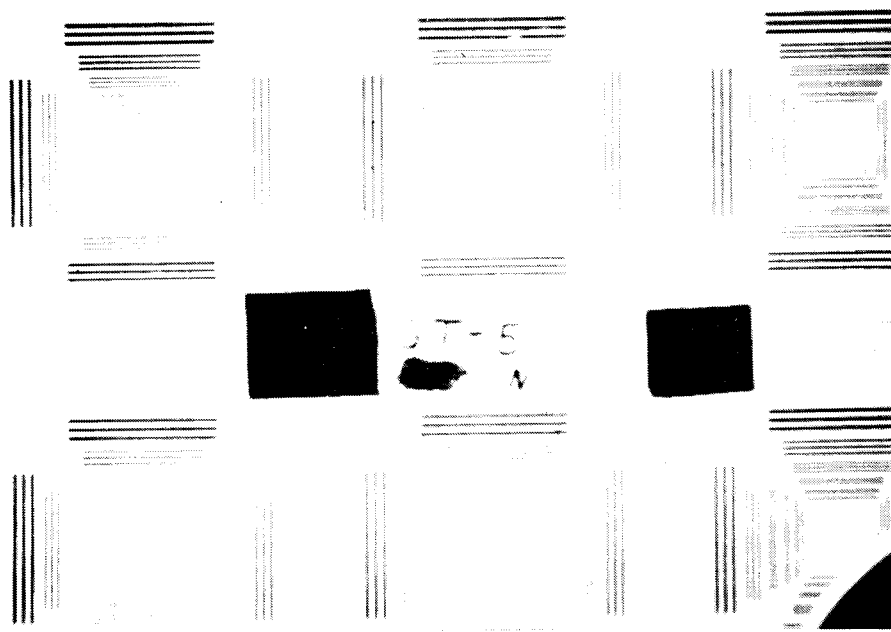


(d) Through clean left window.

Figure 11. - Concluded.

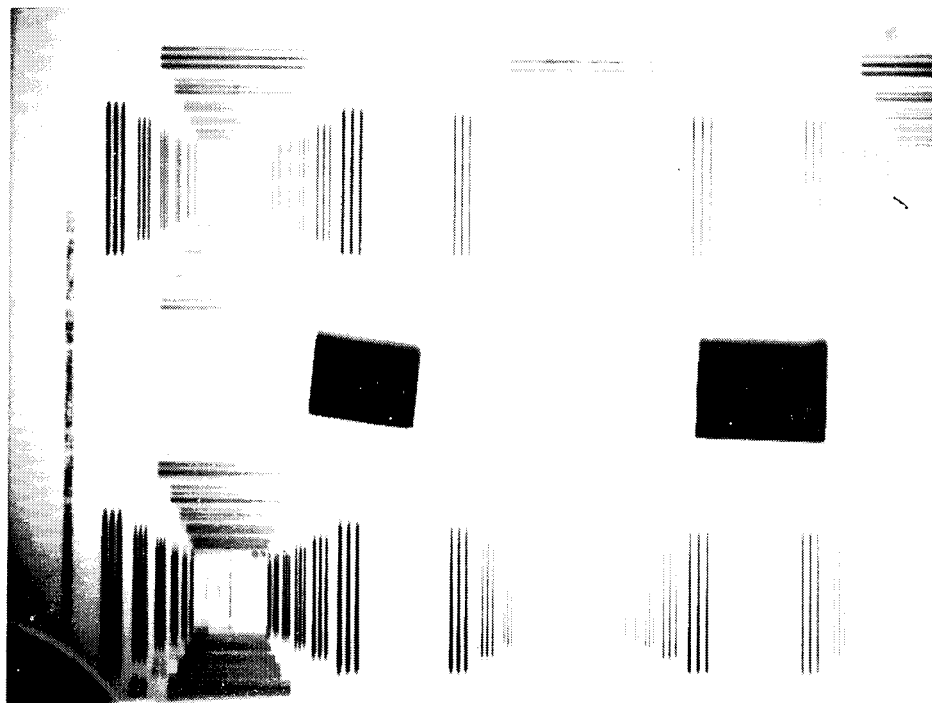


(a) Through dirty right window.

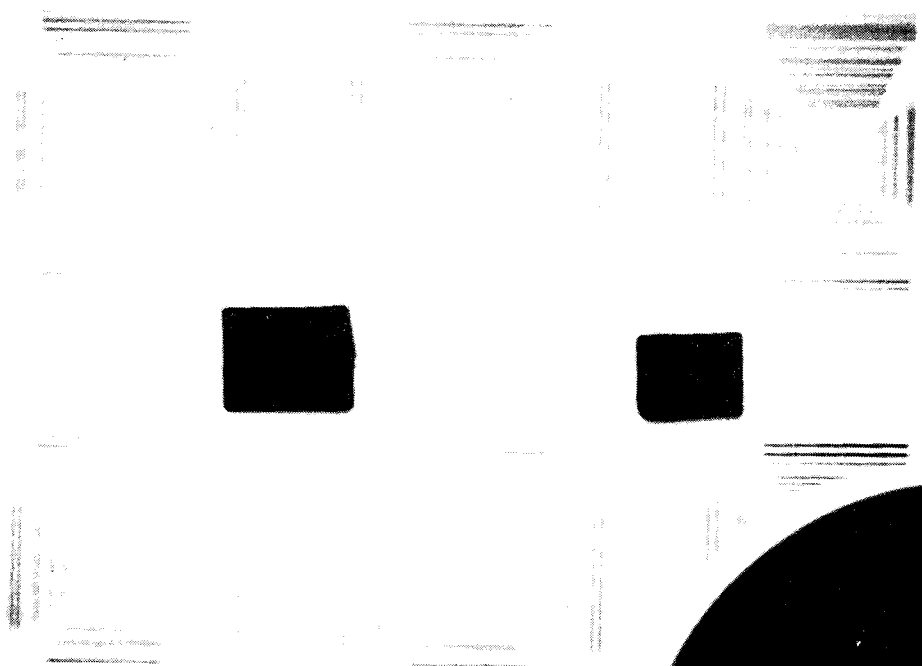


(b) Through clean right window.

Figure 12. - Photographs of NBS resolution charts, G-V.

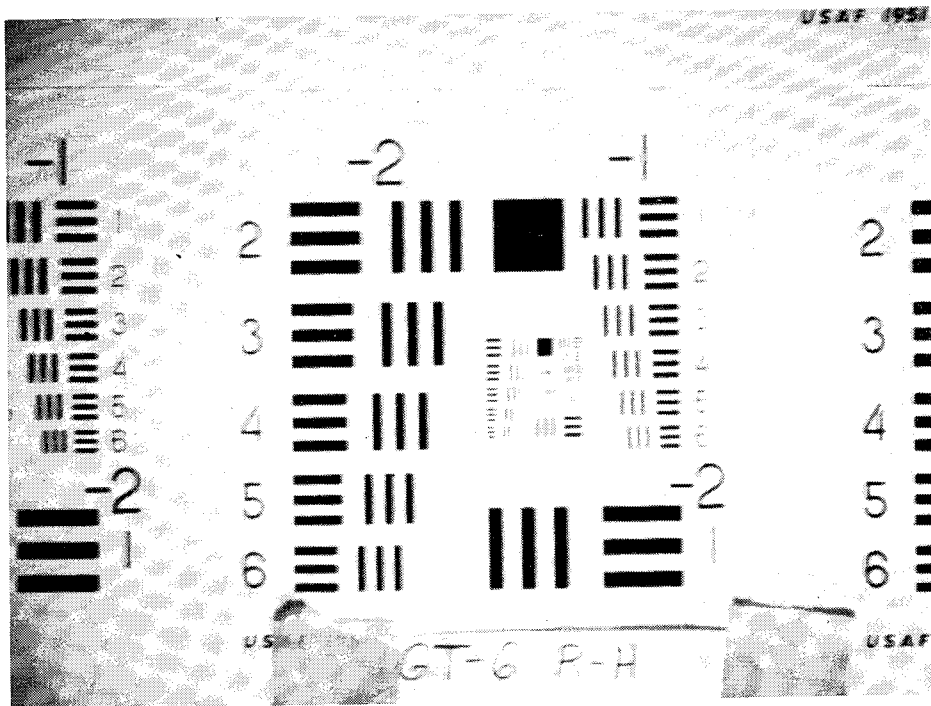


(c) Through dirty left window.

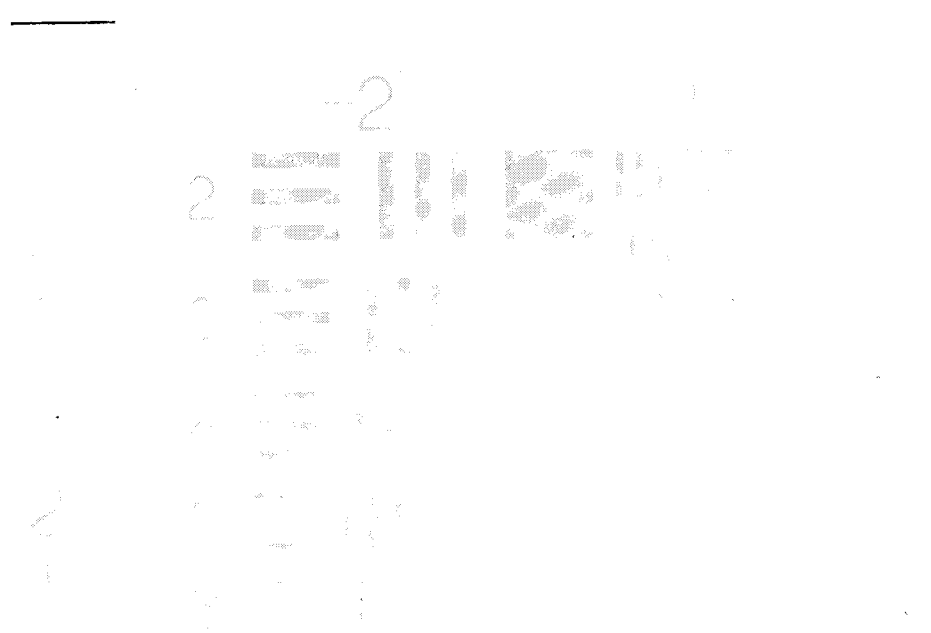


(d) Through clean left window.

Figure 12. - Concluded

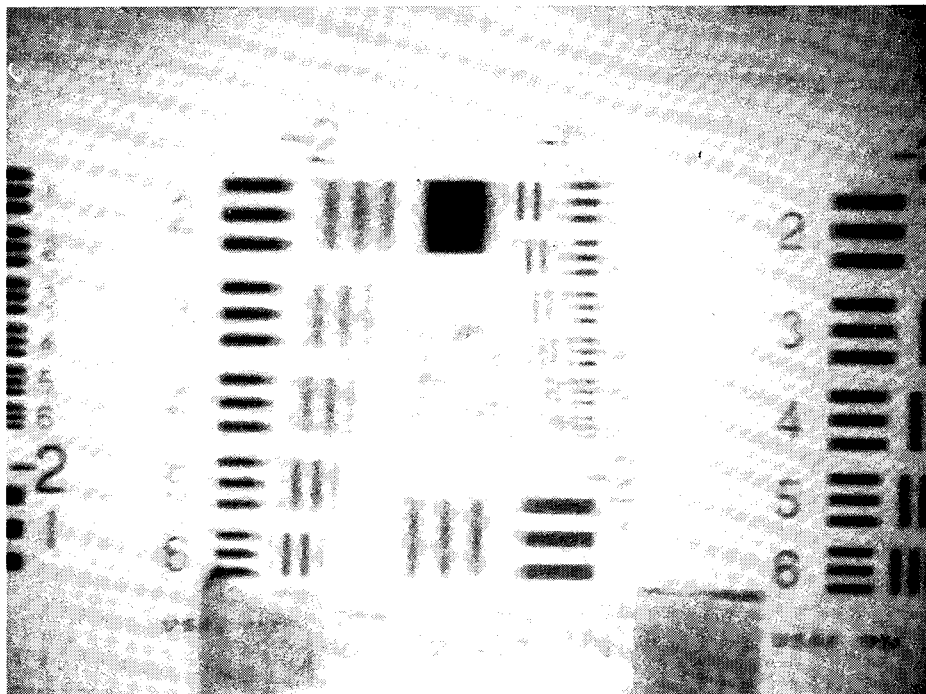


(a) Through dirty right window.

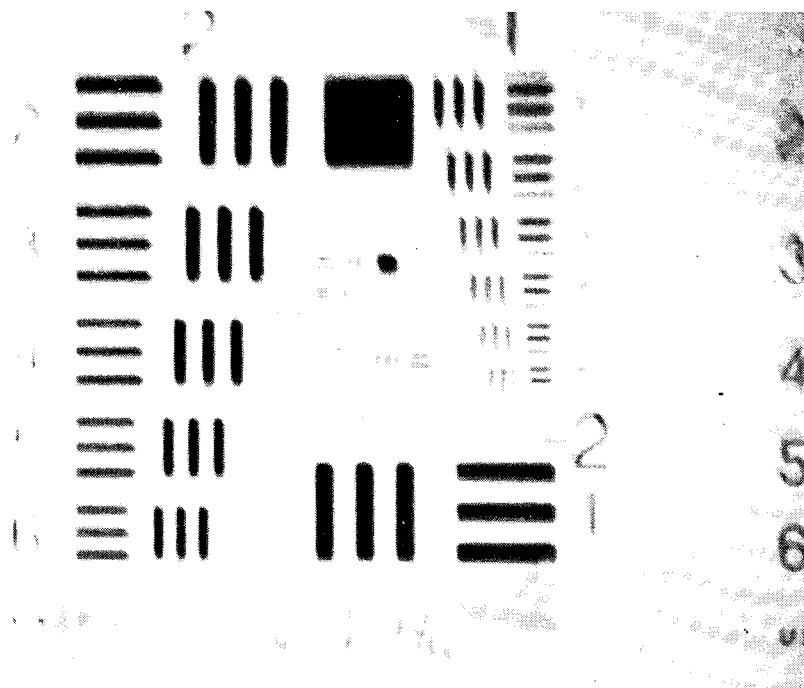


(b) Through clean right window.

Figure 13. - Photographs of USAF bar charts, G-VI.

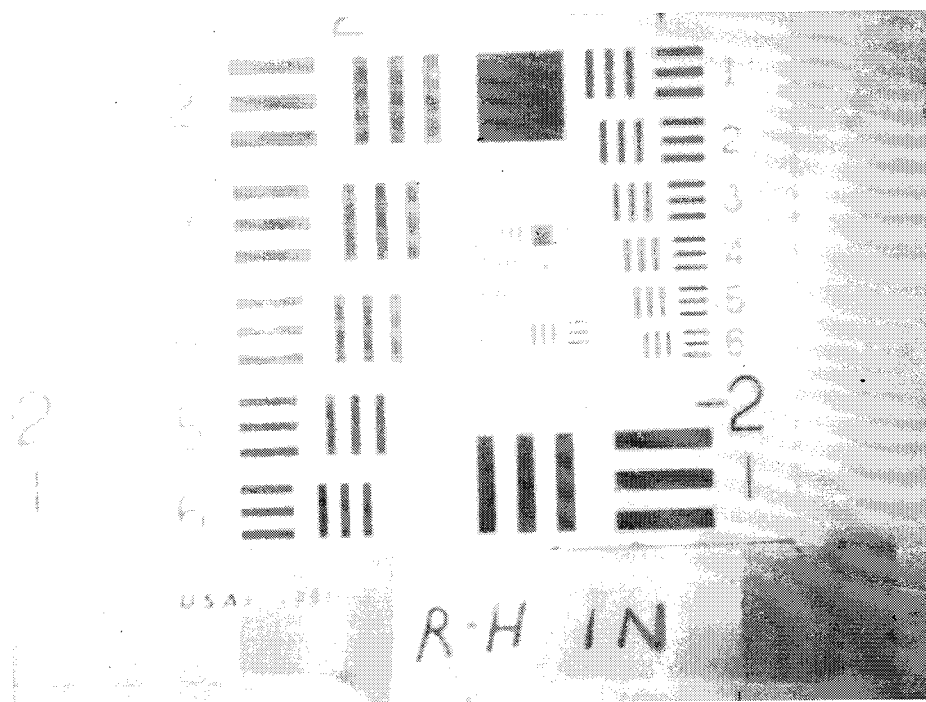


(c) Through dirty left window.

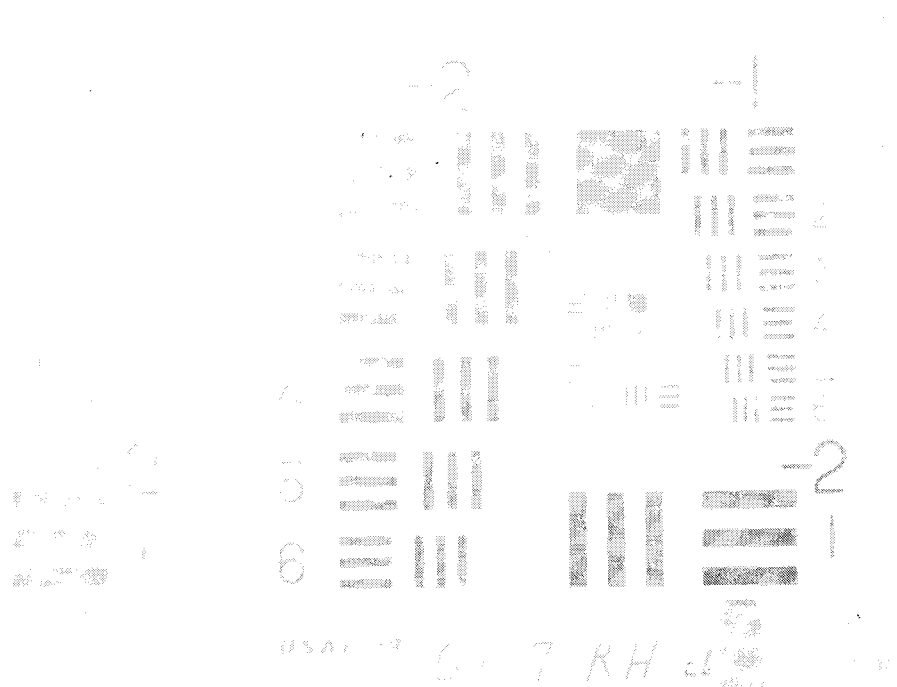


(d) Through clean left window.

Figure 13. - Concluded.



(a) Through dirty right window.



(b) Through clean right window.

Figure 14. - Photographs of USAF bar charts, G-VII.

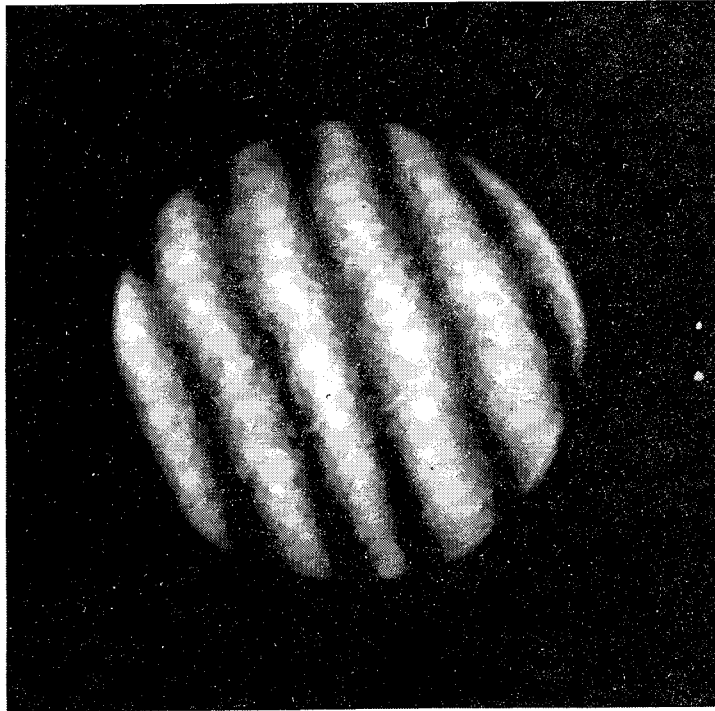


(c) Through dirty left window.

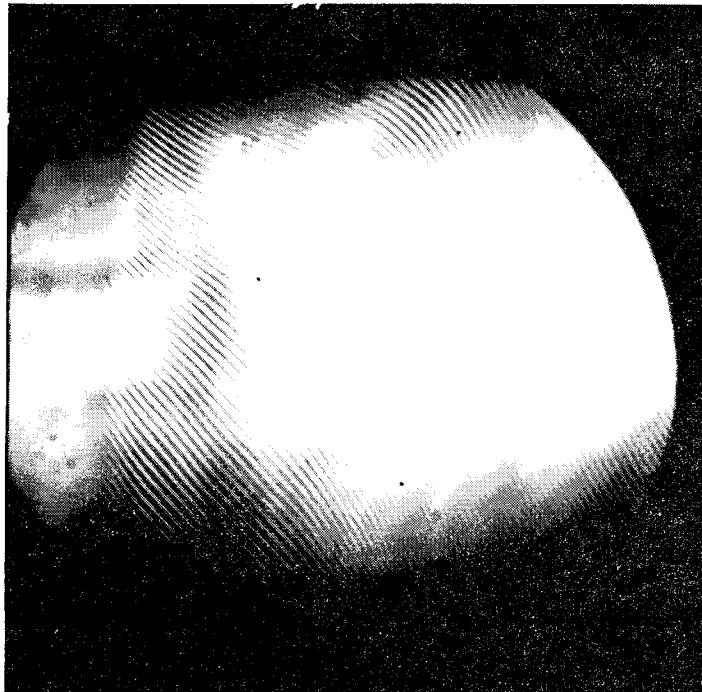


(d) Through clean left window.

Figure 14. - Concluded.

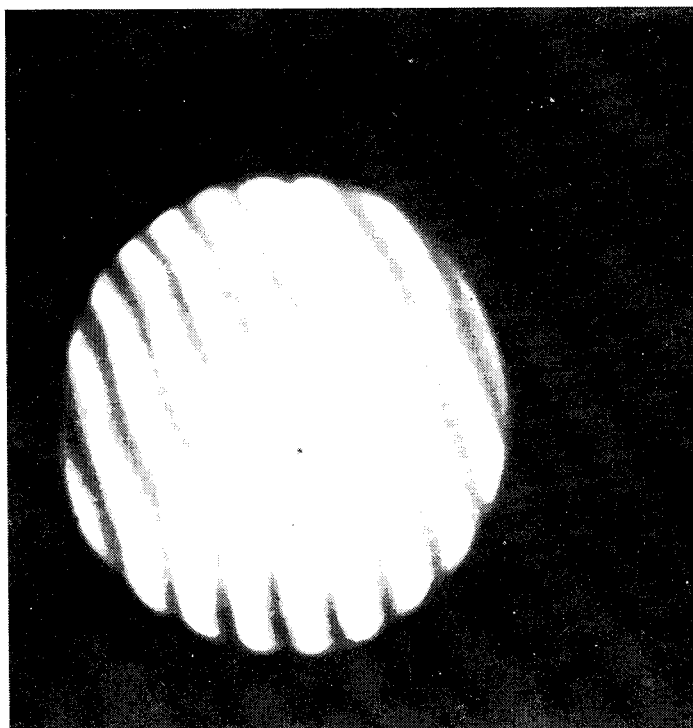


(a) Clean right window.

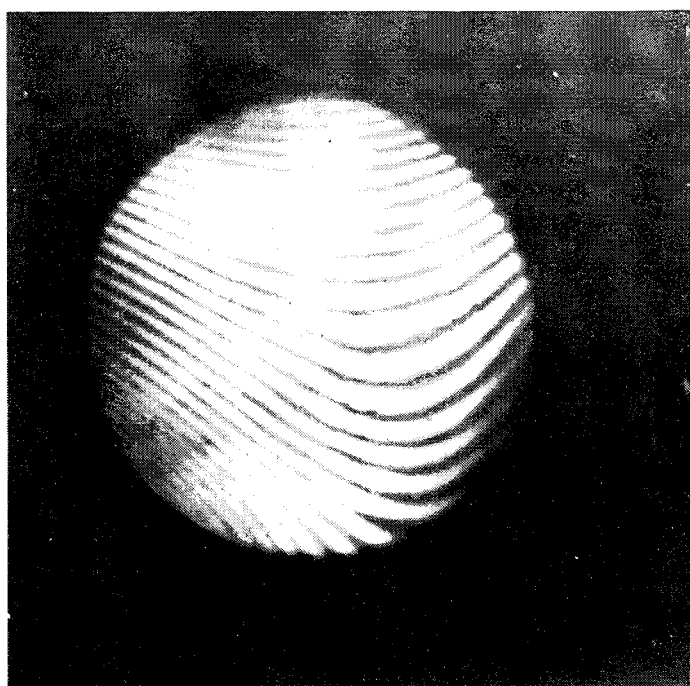


(b) Clean left window.

Figure 15. - Interferograms, G-IV.

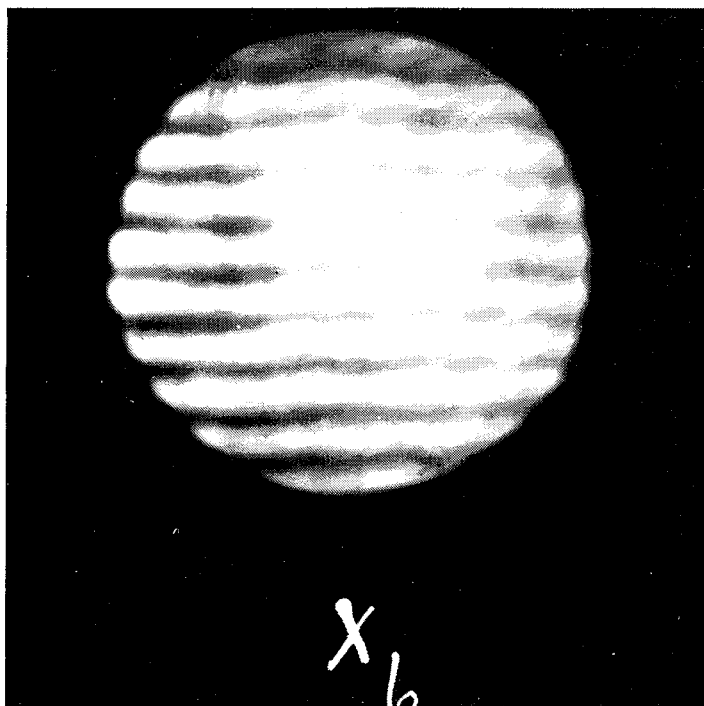


(a) Clean right window.

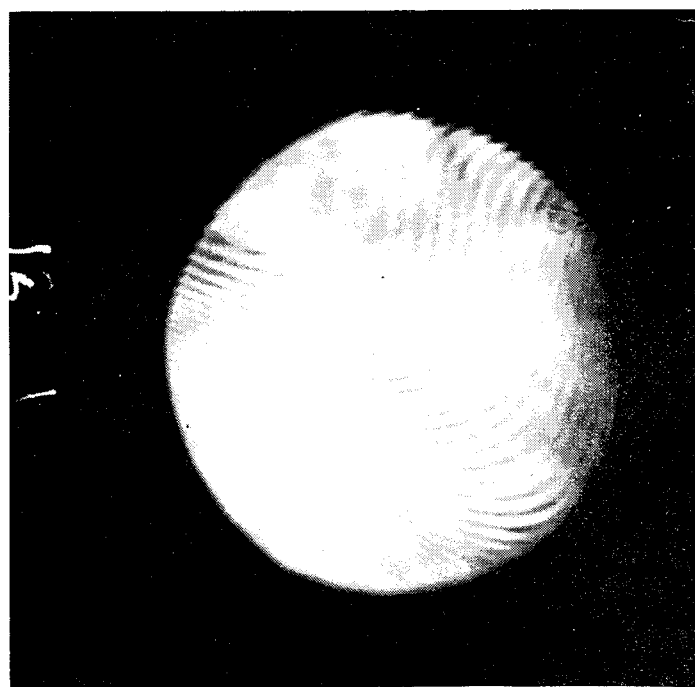


(b) Clean left window.

Figure 16. - Interferograms, G-V.

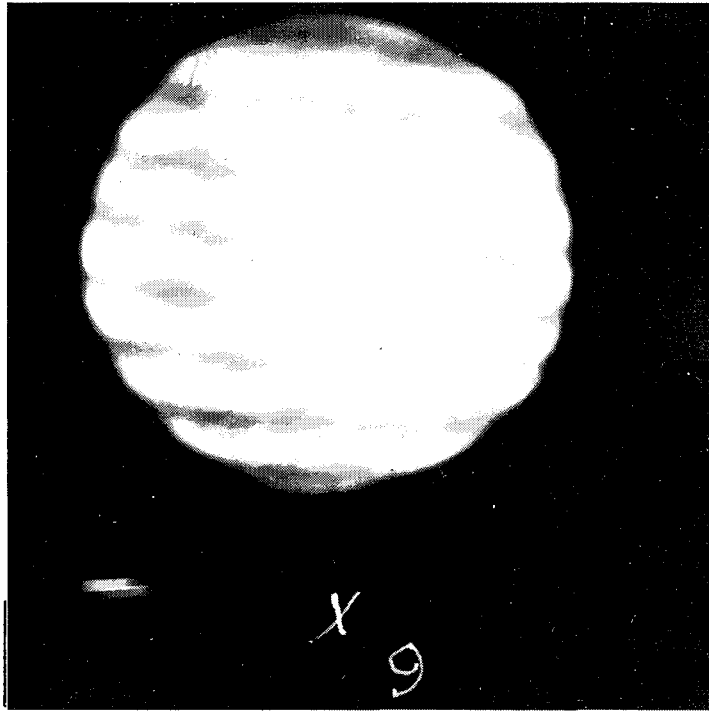


(a) Clean right window.

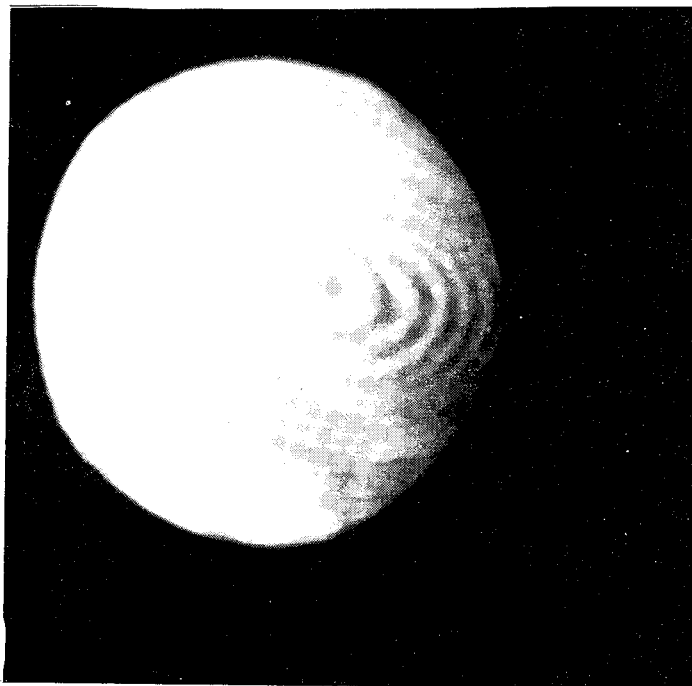


(b) Clean left window.

Figure 17. - Interferograms, G-VI.



(a) Clean right window.



(b) Clean left window.

Figure 18. - Interferograms, G-VII.

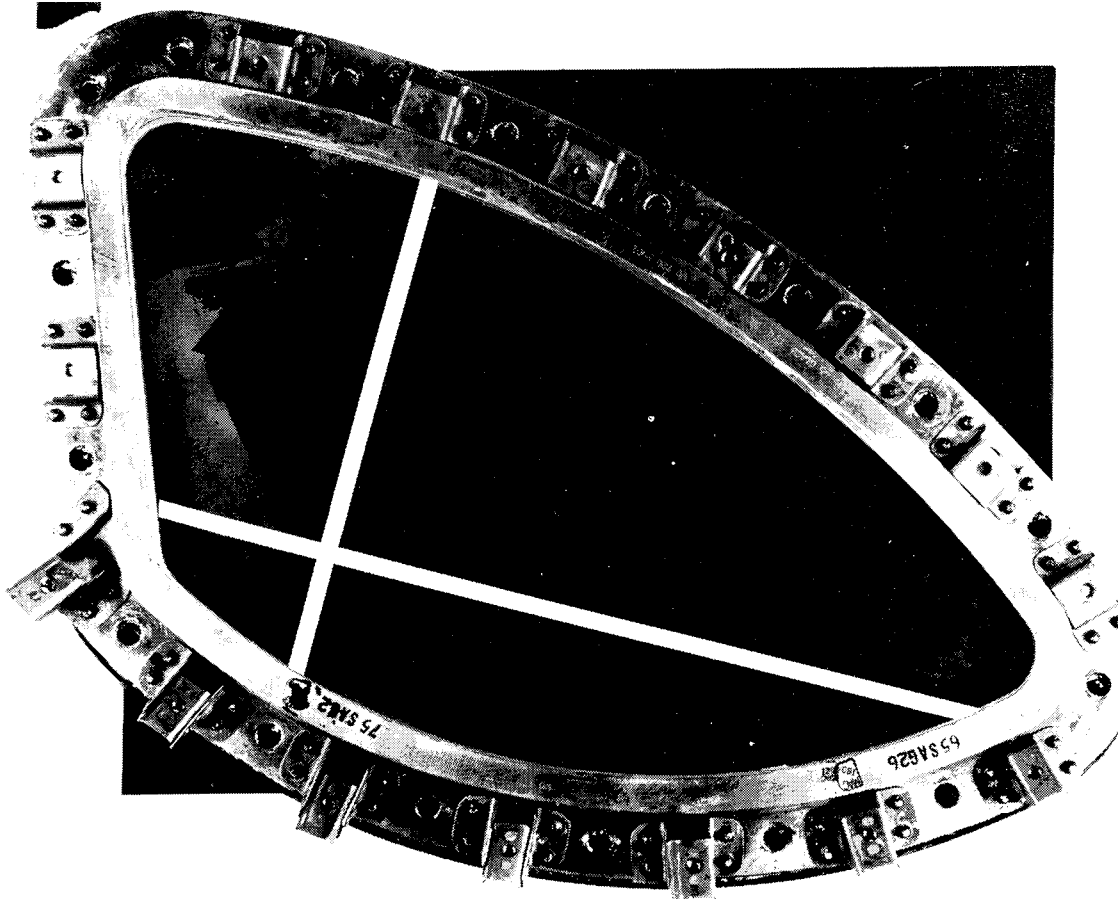


Figure 19. - Location of vertical and lateral scans on right windows.

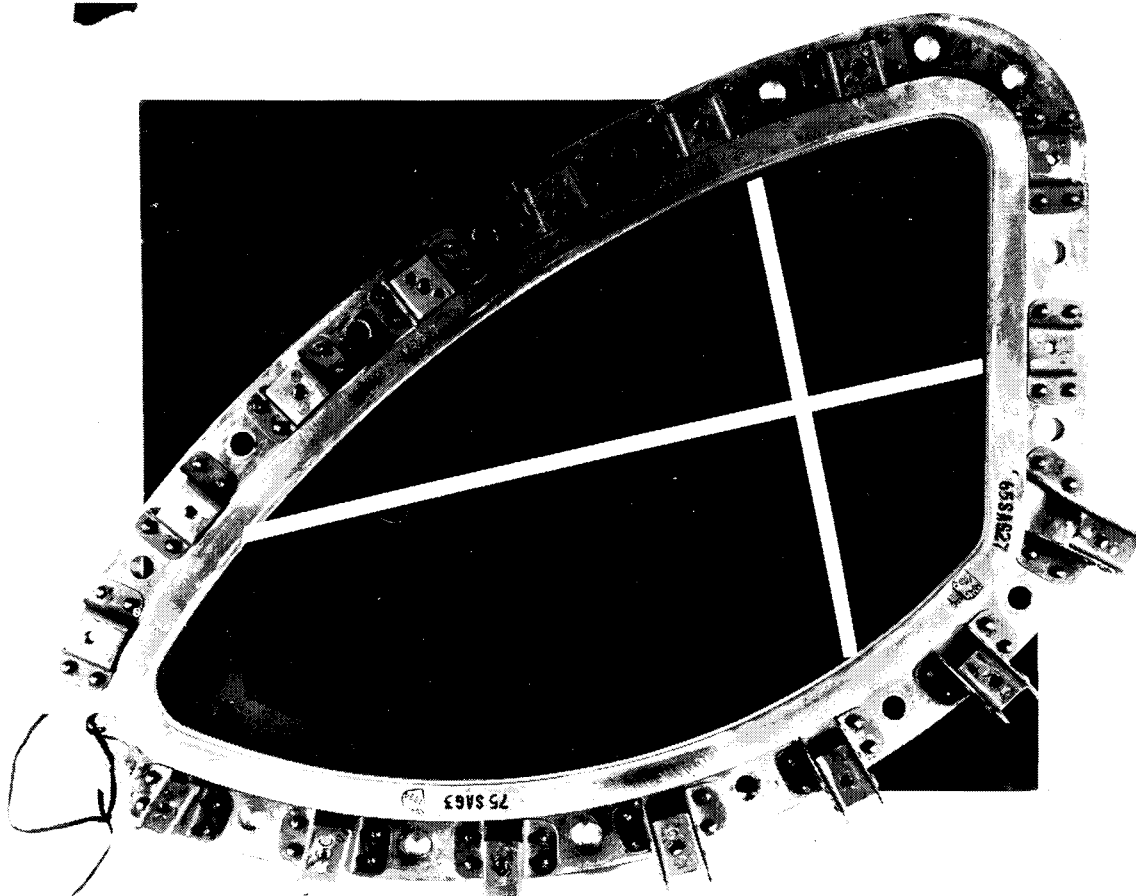


Figure 20. - Location of vertical and lateral scans on left windows.

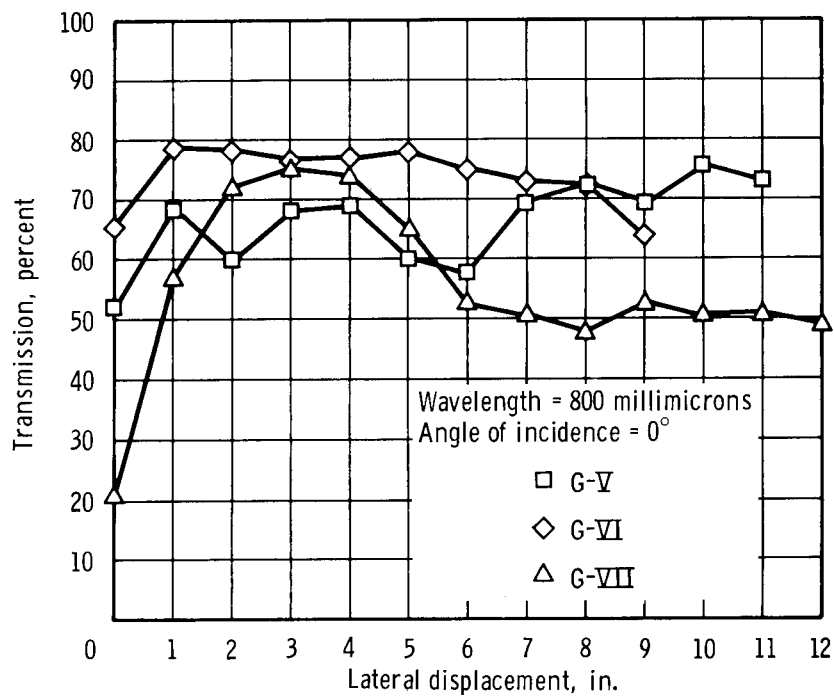


Figure 21. - Percent transmission versus lateral displacement of dirty right window for G-V, G-VI, and G-VII.

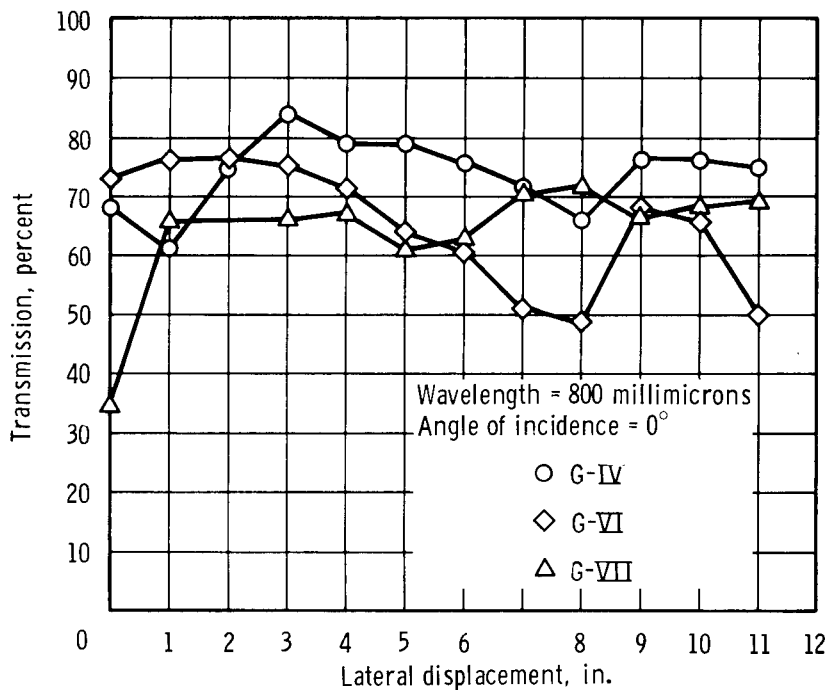


Figure 22. - Percent transmission versus lateral displacement of dirty left window for G-IV, G-VI, and G-VII.

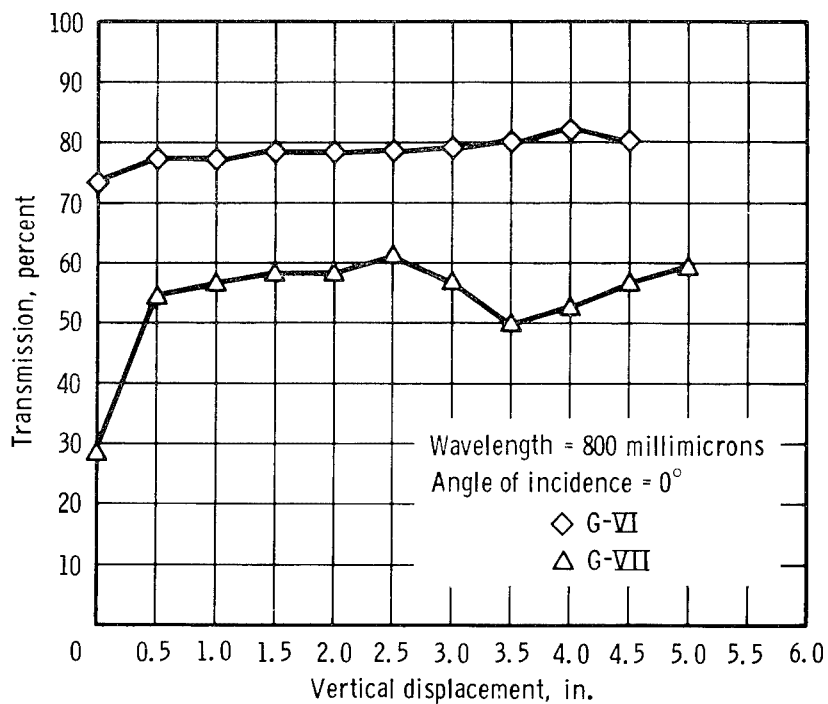


Figure 23. - Percent transmission versus vertical displacement of dirty right window for G-VI and G-VII.

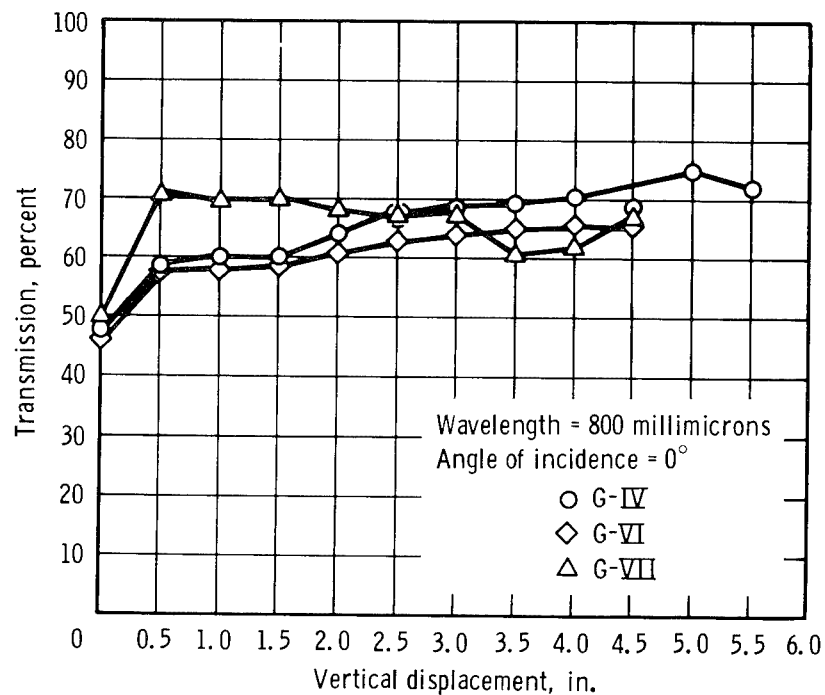


Figure 24. - Percent transmission versus vertical displacement of dirty left window for G-IV, G-VI, and G-VII.

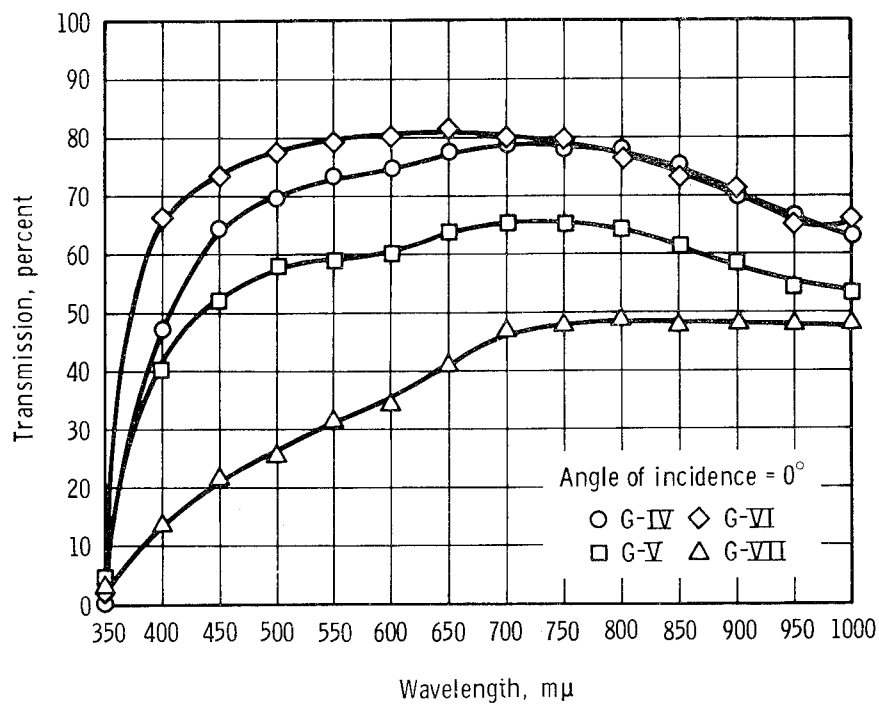


Figure 25. - Percent transmission versus wavelength of dirty right window for G-IV to G-VII.

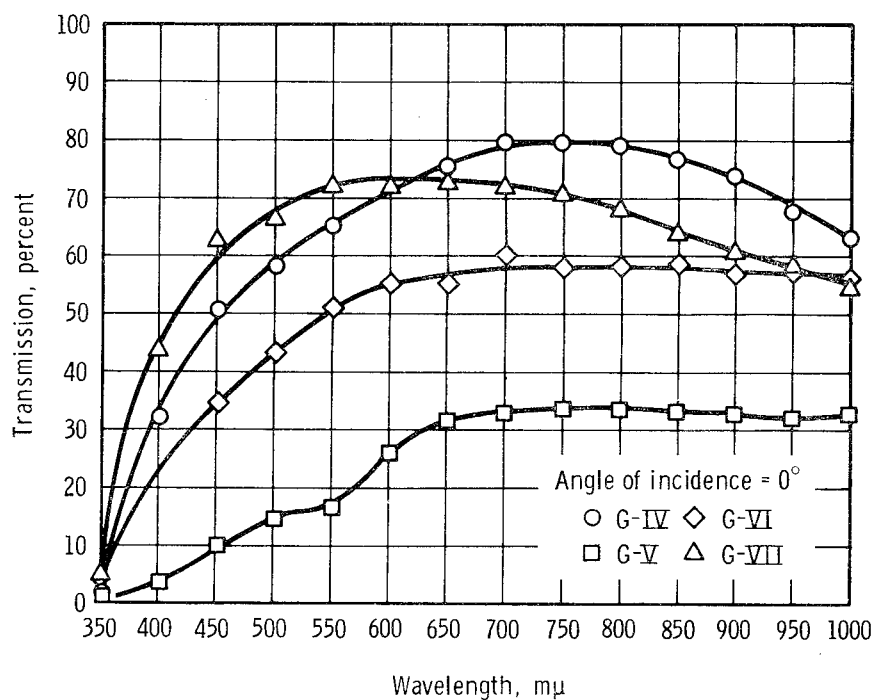


Figure 26. - Percent transmission versus wavelength of dirty left window for G-IV to G-VII.

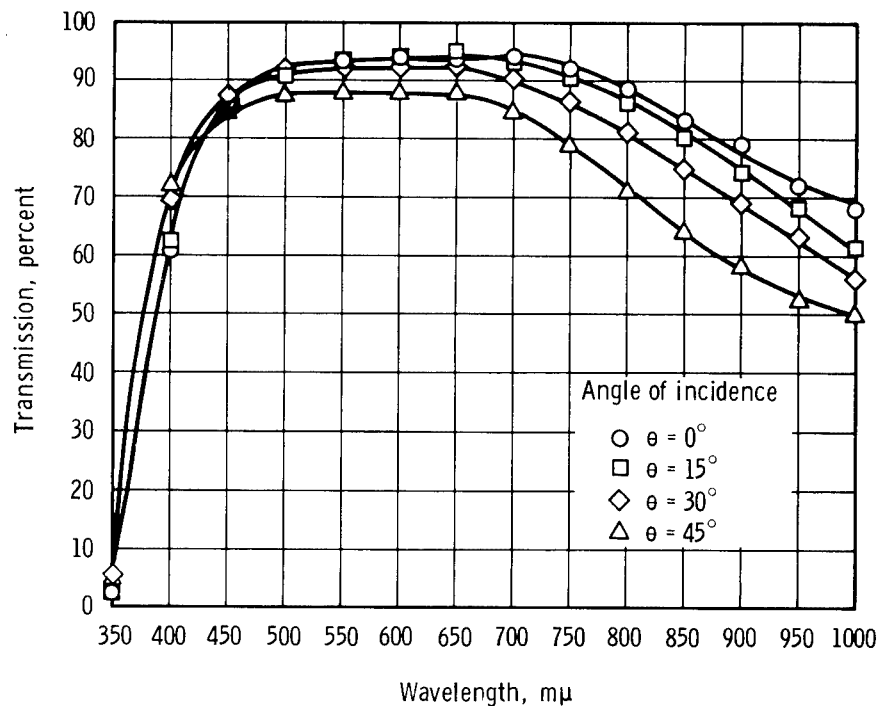


Figure 27. - Percent transmission versus wavelength and angle of incidence for clean right window.

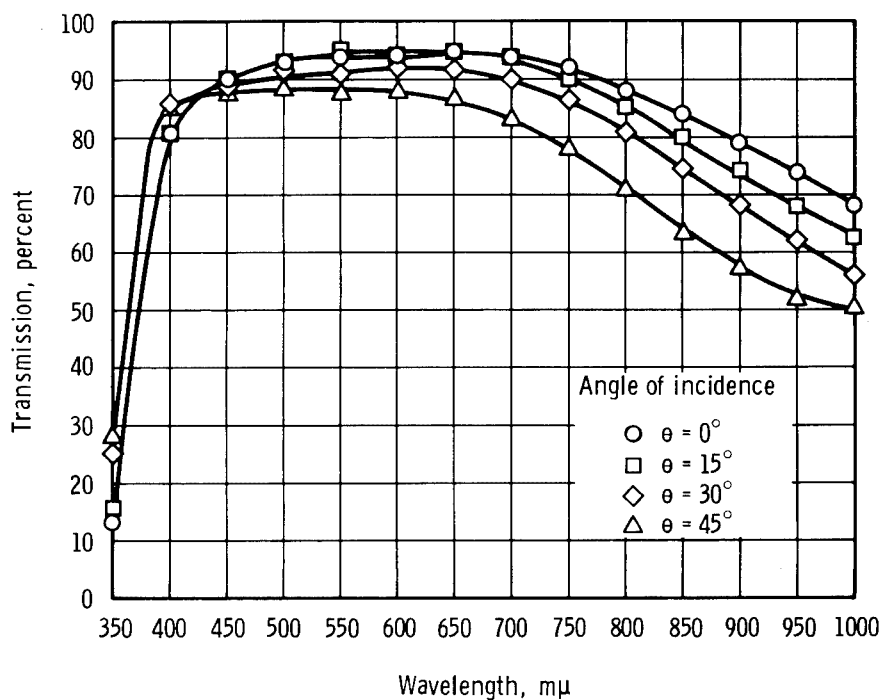


Figure 28. - Percent transmission versus wavelength and angle of incidence for clean left window.